Praca wykonana w ramach projektu TEAM kierowanego przez Prof. Pawła Moskala. Projekt finansowany przez Fundację na rzecz Nauki Polskiej.

Jagiellonian University in Krakow

Faculty of Physics, Astronomy and Applied Computer Science

Development of experimental conditions for measuring the ortho-positronium lifetime in extracellular vesicles obtained in vitro

Julia Nizioł

Student number: 1160270

Master's thesis

field of study: Biophysics

Thesis written under the supervision of

prof. dr hab. n. med. Ewa Łucja Stępień

Department of Medical Physics

Kraków 2023

Oświadczenie autora pracy

Świadom odpowiedzialności prawnej oświadczam, że niniejsza praca dyplomowa została napisana przeze mnie samodzielnie i nie zawiera treści uzyskanych w sposób niezgodny z obowiązującymi przepisami.
Oświadczam również, że przedstawiona praca nie była wcześniej przedmiotem procedur związanych z uzyskaniem tytułu zawodowego w wyższej uczelni.

.....	.....
Kraków, dnia	Podpis autora pracy

Oświadczenie kierującego pracą

Potwierdzam, że niniejsza praca została przygotowana pod moim kierunkiem i kwalifikuje się do przedstawienia jej w postępowaniu o nadanie tytułu zawodowego.

.....	.....
Kraków, dnia	Podpis kierującego pracą

First and foremost I would like to express my sincere gratitude to my supervisor, ***Prof. Ewa Stępień****, for suggesting the topic of this thesis and for her help in every stage of the research and thesis preparation. I also thank* ***Prof. Paweł Moskal*** *for his insightful comments and suggestions and for the studentship that allowed me to conduct this thesis. Working in Prof. Stępień's and Prof. Moskal's research group aroused my interest in the subject of Positronium Lifetime Spectroscopy and allowed me to enter the fascinating world of biomedical research.*

I would like to offer my special thanks to ***Miss Carina Rząca*** *who was always ready to help me with the experimental work and whose experience and kind words made completing this thesis much easier and more enjoyable.*

I also greatly appreciate all the support I received from ***Dr Szymon Niedźwiecki*** *and* ***Dr Ewelina Kubicz****.*

This work was supported by the Foundation for Polish Science through the
TEAM POIR.04.04.00-00-4204/17 programme and OPUS 17 grant no. 2019/33/B/NZ3/01004.

Contents

Abstract

Investigating the ortho-positronium (o-Ps) lifetime in biological materials holds promise for enhancing our understanding of biological processes and pathologies. This master's thesis aimed to develop experimental conditions for the measurement of the o-Ps lifetime in extracellular vesicles (EVs) isolated using the low-pressure filtration method. EVs in question were derived from a large-scale 2D human pancreatic beta cell culture (1.1B4 cell line) maintained under normoglycemic conditions.

In order to check the effectiveness of the chosen method of isolation, environmental scanning electron microscopy (ESEM) images of the dialysis membrane were taken, which allowed to determine the size of its pores. Fourier transform infrared spectroscopy (FTIR) was employed to characterise the chemical composition of EVs. The qNano device, which operates on the principle of tunable resistive pulse sensing (TRPS), was used to determine the size distribution and concentration of EVs. Transmission electron microscopy (TEM) was employed to visualise the morphological features of EVs and validate their structural integrity. Finally, positron annihilation lifetime spectroscopy (PALS) was used to investigate the o-Ps lifetime in the EV sample. In addition, the PALS technique was also used to study the lifetime of o-Ps in pancreatic beta cells from which the vesicles were derived, and in PBS buffer in which they were suspended after the isolation. The o-Ps lifetime and intensity for the sample containing EVs measured at 22°C were 1.87 ns and 15.4%. The same sample investigated at 34.2 °C gave results of 1.83 ns and 15.0%, respectively. These results were not significantly different from the results of the PBS measurement.

This study allowed to test several technical solutions to measure the positronium lifetime in EV samples. It underscores the need for continued efforts in exploring EVs with progressive methods such as PALS, as they hold immense potential, for example as carriers of biological cargo or biomarkers.

Streszczenie

Badanie czasu życia orto-pozytonium (o-Ps) w materiałach biologicznych może przyczynić się do lepszego zrozumienia zachodzących procesów, zarówno tych prawidłowych jak i patologicznych. Niniejsza praca magisterska miała na celu opracowanie warunków doświadczalnych do pomiaru czasu życia o-Ps w pęcherzykach zewnątrzkomórkowych (EVs) wyizolowanych metodą filtracji niskociśnieniowej. Omawiane EVs pochodziły z hodowli 2D ludzkich komórek beta trzustki (linia komórkowa 1.1B4) prowadzonej na dużą skalę i utrzymywanej w warunkach normoglikemicznych. W badaniach wykorzystano kilka technik analitycznych.

W celu sprawdzenia skuteczności wybranej metody izolacji wykonano zdjęcia membrany dializacyjnej za pomocą środowiskowej skaningowej mikroskopii elektronowej (ESEM), co pozwoliło określić wielkość jej porów. Technikę spektroskopii w podczerwieni z transformacją Fouriera (FTIR) wykorzystano w celu scharakteryzowania składu chemicznego EVs. Urządzenie qNano, które działa na zasadzie TRPS (Tunable Resistive Pulse Sensing), zostało użyte do określenia rozkładu wielkości i koncentracji EVs w próbce. Wykorzystano również transmisyjną mikroskopię elektronową (TEM) do wizualizacji cech morfologicznych EVs i sprawdzenia ich prawidłowej struktury. Kluczowym etapem badań było przygotwanie układu i wykonanie pomiarów tehcniką spektroskopii czasu życia pozytonów (PALS) badając w ten sposób czas życia o-Ps w próbce EVs. Ponadto technikę PALS zastosowano również do określenia czasu życia o-Ps w komórkach beta trzustki, z których pochodzą pęcherzyki, oraz w buforze PBS, z którego wykonano zawiesinę EVs po ich izolacji. Czas życia i intensywność o-Ps dla próbki zawierającej EVs zmierzone w temperaturze 22°C wyniosły 1.87 ns i 15.4%. Ta sama próbka zbadana w temperaturze 34.2°C dała odpowiednio wyniki 1.83 ns i 15.0%. Wyniki te nie różniły się w sposób istotny statystycznie od wyników pomiaru PBS.

Badania opisane w tej pracy pozwoliły na sprawdzenie szeregu technicznych rozwiązań istotnych dla pomiaru czasu życia pozytonium w próbkach EVs. Podkreślają one potrzebę ciągłego poznawania EVs z wykorzystaniem progresywnych metod, takich jak PALS, z racji na ogromny potencjał ich zastosowań m.in. jako systemy dostarczania leków czy biomarkery.

List of Abbreviations

A	attenuator
ATR	attenuated total reflectance
CFD	constant fraction discriminator
CON	coincidence module
DNA	deoxyribonucleic acid
EDTA	ethylenediaminetetraacetic acid
ESEM	environmental scanning electron microscopy
EVs	extracellular vesicles
FBS	fetal bovine serum
FTIR	fourier transform infrared spectroscopy
HSP	heat shock protein
IAPP	islet amyloid polypeptide
ILVs	intraluminal vesicles
LVED	low vacuum electron detector
MVBs	multivesicular bodies
NG	normoglycemia
o-Ps	ortho-Positronium
PALS	positron anihilation lifetime spectroscopy
PBS	phosphate buffered saline
PC	phospatidylcholine
PET	positron emission tomography

PHM photomultiplier

PM plasma membrane

p-Ps para-Positronium

PS phosphatidylserine

Ps Positronium

RNA ribonucleic acid

TEM transmission electron microscopy

TRPS tunable resistive pulse sensing

List of reagents

Reagent	Vendor	Cat. No.
RPMI 1640 medium	Gibco™	21875091
10% Fetal Bovine Serum	Gibco™	10500064
2mM L-Glutamine	Gibco™	25030081
100 U/mL Penicillin and 100 mg/mL Streptomycin	Gibco™	15140122
PBS without Ca^{2+}, Mg^{2+}	Gibco™	10010015
0.25% trypsin - EDTA	Gibco™	25200072
2.5% glutaraldehyde solution	Sigma-Aldrich	G5882
0.1 M cacodylic buffer	Sigma-Aldrich	C4945

1. Introduction

1.1 Extracellular vesicles

Extracellular Vesicles (EVs) are lipid-bound vesicles secreted by various cells into the extracellular space both in vitro and in vivo. They have been reported in virtually all human biological fluids, including blood, lymph, and nasal mucus [1][2][3] [4][5][6][7][8]. These small (30 nm - 5 µm) spherical structures surrounded by a lipid bilayer differ not only in size but also in the mechanism of their release and the cargo they carry, as shown in Table 1. Extracellular vesicles are most

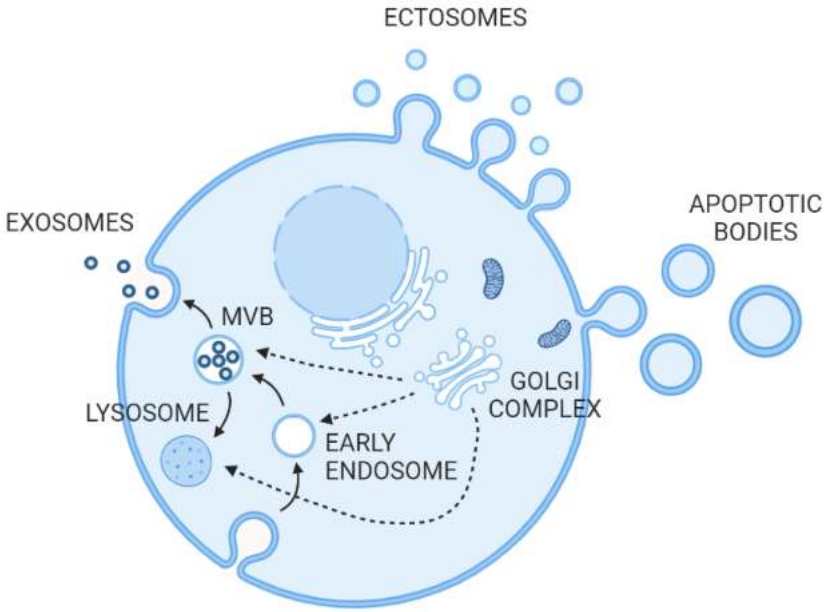

Figure 1. Formation and release of different types of EVs [created with BioRender.com].

often grouped based on their size or biogenesis. We distinguish three types of EVs: small extracellular vesicles (exosomes), ectosomes, and apoptotic bodies (Table 1). You can also come across a slightly different nomenclature, where ectosomes are called microvesicles or microparticles.

The smallest of EVs - exosomes, can be formed as a result of the inward budding of the limiting membrane of endosomes, via the creation of multivesicular bodies (MVBs). MVBs contain intraluminal vesicles (ILVs) - the precursors of exosomes. Subsequently, exosomes are released into the extracellular space by the fusion of MVBs with the plasma membrane (PM). Following release from the cell surface (exocytosis), exosomes can interact with the extracellular matrix, or elicit a response in cells within the microenvironment or at a distance [9]. Exosomes

Table 1. Characterization of EV populations according to diameter, biogenesis, physiological role, cargo, and typical markers [6].

	Small extracellular vesicles	Microvesicles	Apoptotic bodies
Diameter	30 - 100 (nm)	100 - 1000 (nm)	1000 - 5000 (nm)
Release mechanism	By formation of intraluminal vesicles (ILVs) in MVBs, transport of MVBs to the PM and fusion of MVBs with the PM	By direct outward budding from the PM	Cell fragments released during cell apoptosis
Role	Cell-to-cell communication	Cell-to-cell communication	Phagocytosis facilitation
Cargo	DNA, RNA, proteins	DNA, RNA, proteins	Cell organelles, nuclear fraction
Markers	Tetraspanins: CD9, CD63, CD81, Hsp70, Hsp90, Alix, Tsg 101, flotilin	Integrins, selectins, Arf-6	Thrombospondin and C3b

are enriched in proteins occurring in multivesicular bodies (Alix, TSG101), as well as heat shock proteins (HSP60, HSP70, HSP90), proteins involved in membrane transport (annexins, flotilins, GTPase), and cell adhesion (integrins). Moreover, the membranes are rich in tetraspanins (CD9, CD63, CD81, CD82) - small transmembrane proteins that are critically important for trapping both membrane and luminal proteins [10]. In their composition, we can also distinguish non-coding RNA, DNA, and lipids such as ceramide, cholesterol, phosphatidylserine (PS), and sphingolipids [5][11][12][13][14][15].

Unlike in exosomes, the release of ectosomes does not require exocytosis. It involves the formation of outward buds in specific regions of the cell membrane, followed by direct shedding and immediate release of the vesicle to the intercellular space [5][9][15]. When considering these two types of EVs, in addition to distinct release mechanisms and different sizes, both their membranes and cargoes slightly differ from each other. Similarly to exosomes, in ectosomes, the membrane consists of different types of lipids such as PS (3.63%), phosphatidylcholine (PC, 59.2%), sphingomyelin (20.6%), phosphatidylethanolamine (PE, 9.4%) and lysophospholipids (<2%) [16]. It also contains additional proteins and is abundant in specific receptors, glycoproteins, and metalloproteinases. The unique composition of the molecules that they carry, and their functional role, depends largely on the state of their originating cell [15]. In the past decades, also

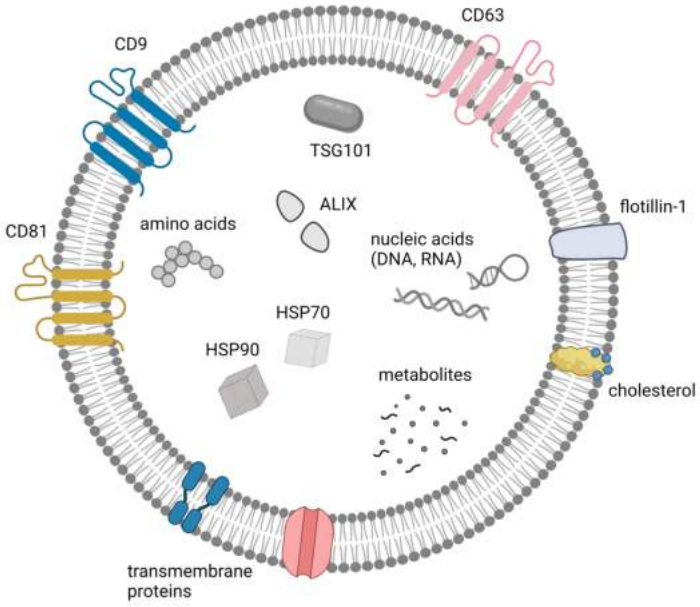

Figure 2. An exemplary structure of an exosome; CD81, CD9, CD63 - various types of glycoproteins, antigens; flotillin-1 - membrane protein; TSG101 - a polypeptide that plays an important role in maintaining genome stability and in regulating the cell cycle; HSP70, HSP90 - proteins from the family of heat shock proteins; ALIX - a protein involved in the regulation of cellular processes such as pro-apoptotic signaling [17][18] [created with BioRender.com].

miRNAs and mRNAs have been found to be major components of EVs [5].

EVs are biologically active, they intrinsically transport cargo between cells, and therefore play a huge role in intercellular communication [19]. They are involved not only in physiological processes such as adhesion, coagulation, angiogenesis, and vascular remodeling but also play pathophysiologic roles in various diseases such as diabetic chronic kidney disease [2][3][5][6][8][12][20]. EVs transfer their cargo to target cells through ligand/receptor interaction, fusion or internalisation, which protects the cargo from enzymatic degradation [21]. Thanks to these properties, EVs can be used as diagnostic indicators. They constitute as a novel class of biomarkers, creating a promising prospect for better diagnostics. EVs are also one of the most prominent examples of natural carriers that can be a more suitable alternative to synthetic drug delivery systems limited due to inefficiency, cytotoxicity, or immunogenicity [9].

1.2 Positronium and Positron Annihilation Lifetime Spectroscopy

Positron Annihilation Lifetime Spectroscopy (PALS) is a non-destructive spectroscopic technique that enables the testing of various materials at the nano and sub-nano scale. PALS uses positrons to probe free volumes in the material. The fundamental operational principle relies on establishing a correlation between the lifetime of the injected positrons and the void size in the sample [22].

The source of positrons in the PALS method is the radioactive β^+ decay of the ^{22}Na isotope:

$$ {}^{A}_{Z}X \rightarrow {}^{A}_{Z-1}Y + e^+ + \nu_e \ , \tag{1} $$

where: A - mass number, Z - atomic number of the decaying nucleus, X - initial element, Y - final element, e^+ - positron, ν_e - neutrino.

The thermalised positron produced during the decay can directly annihilate with one of the electrons in the medium or create positronium (Ps) - a bound state of a positron and an electron [23][25]. Its creation can be described by considering the so-called 'blob model', in which spherical blobs are formed when a positron loses its kinetic energy due to ionisation and excitation of material's molecules [24][25]. Similarly to how an electron and a proton combine to form hydrogen, the result of electron's combination with its antiparticle - a positron, is a meta-stable Ps atom that exists in two spin states: singlet and triplet.

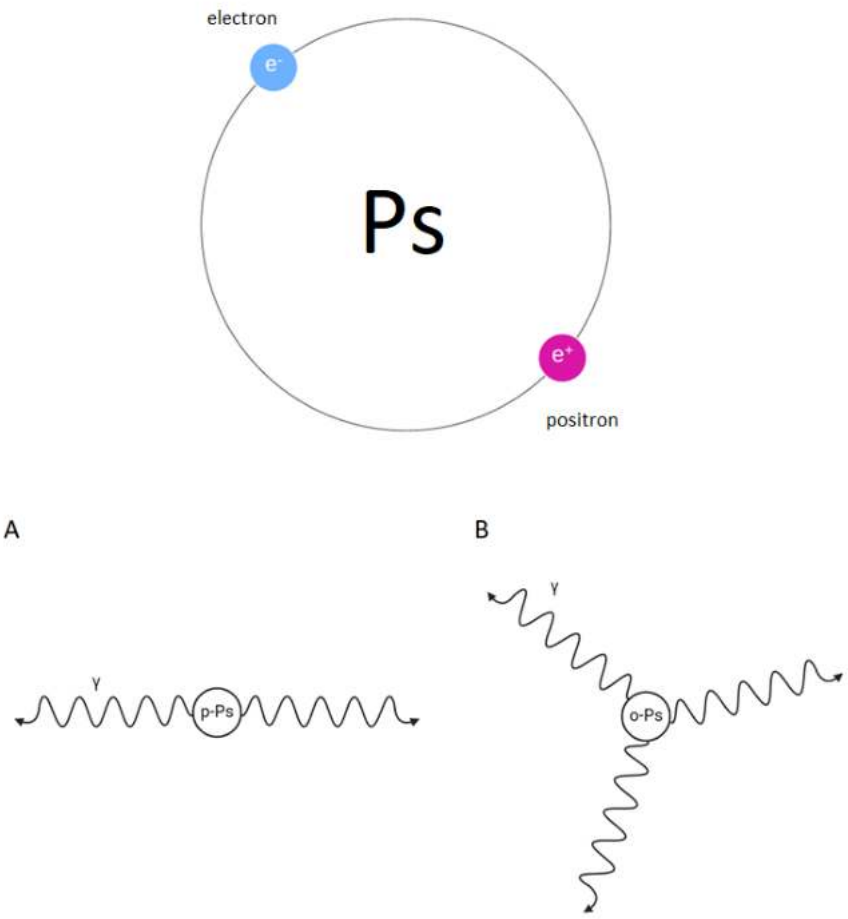

Figure 3. Simplified diagram of a positronium atom. Below are diagrams of decay into two γ quanta (each with 511 keV energy) propagating at an angle of 180 degrees for p-Ps (A) and three γ quanta for o-Ps (B). The energy and angles between γ rays follow the laws of conservation of energy and momentum.

The singlet state, also called para-positronium (para-Ps; p-Ps), occurs when the orientation of positron's and electron's spins are antiparallel (↑↓), resulting in a total spin equal to zero. The p-Ps lifetime is very short (125 ps in vacuum). Positronium in this state usually decays into two gamma quanta, spreading at an angle of 180 degrees (Fig. 3A). The process of direct annihilation of a positron with an electron from the surrounding material will proceed in a similar way without forming a bound state:

$$e^- + e^+ \rightarrow \gamma + \gamma \tag{2}$$

Ortho-positronium (ortho-Ps; o-Ps), i.e. the triplet state, is characterised by a longer average lifetime (142 ns in vacuum) [25]. The spin of such a system is non-zero and equals $\hbar$, due to the parallel spins (↑↑) of particles composing the Ps. As a result of annihilation three gamma quanta may be emitted (Fig. 3B). Ortho-Ps annihilates mainly through collisions with the electrons of the surrounding medium, what we call a pick-off process (pick-off annihilation) [25]. The relatively

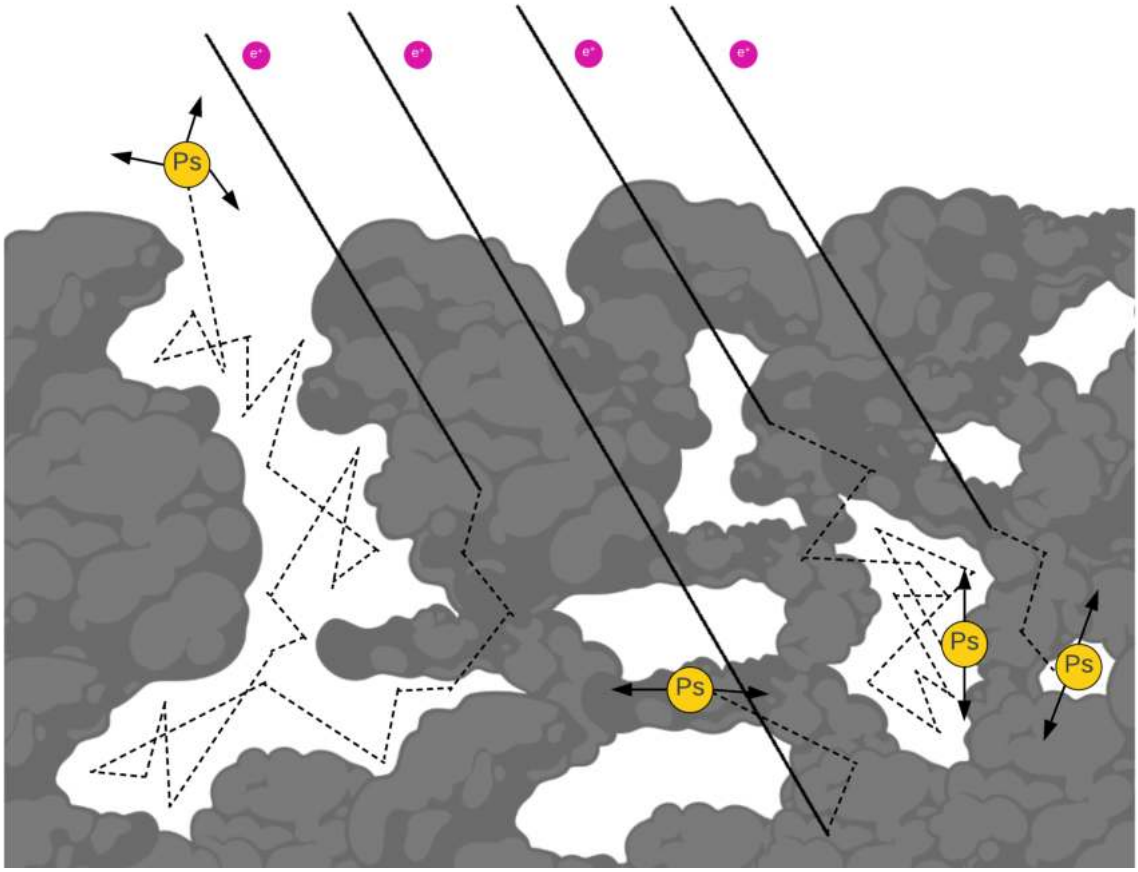

Figure 4. In materials with structure that is characterised by the presence of free volumes, positrons form a quasi-bonded state with electrons (Ps). As a result of the pick-off processes, Ps is finally annihilated with the electron of neighbouring atoms, which usually occurs within a few ns. This process can be correlated with the magnitude of the radius of the free volume using the semi-empirical Tao-Eldrup equation [26].

long lifetime of o-Ps in a vacuum can be shortened in the medium, resulting in values even below 1 ns, due to the possibility of the positronium trapping in the regions of lower electron density

[25]. The formation of positronium can occur only in areas with low or zero electron density, i.e. in the so-called free volumes or voids [25]. The lifetime of o-Ps is a direct measure of the size of these voids due to the occurrence of the pick-off annihilation, whereas the number of free volume elements present can be determined from the o-Ps intensity [27]. PALS is a technique often used to study materials such as polymers and other porous materials [28], although Ps is also formed in liquids, which indicates the possibility of using this phenomenon to study biological samples, such as aqueous solutions or biological membranes and tissues [24][27][29][30]. In the free volumes between the particles, the average lifetime o-Ps decreases to a value of several nanoseconds. The changing lifetime of o-Ps allows the observation of even very small changes in the structure of the sample, which is an immensely promising prospect in the context of biomedical research [25].

2. Thesis goal

The aim of this thesis was to develop a method for determining the mean ortho-positronium lifetime in EVs derived from the 1.1B4 cell line. The starting point was to obtain a sample of EVs from a 2D culture medium of human beta-pancreatic cells and to analyse the obtained sample using different biophysical techniques. The research employs a comprehensive approach integrating Fourier transform infrared spectroscopy (FTIR), nanoparticle tracking analysis (qNano), transmission electron microscopy (TEM), and positron annihilation lifetime spectroscopy (PALS).

This study seeks to enhance our understanding of the behaviour and potential applications of o-Ps in EVs, contributing to the advancement of biomedical research and diagnostic methodologies.

Determining the positronium lifetime within EVs can contribute to understanding their structural characteristics and stability. Investigating the properties of these biological carriers, including their composition and behavior, can provide insights into cellular processes and potential applications in various fields, such as diagnostics, regenerative medicine, and drug delivery.

The PALS technique is still used to a relatively small extent when it comes to studies of biological samples. Such research involves a number of challenges that in this thesis I attempted to overcome in order to provide an accurate sample characterisation of EVs.

3. Materials and methods

3.1 1.1B4 cells and cell culture

EVs which are the subject of the research described in this thesis were obtained from the 1.1B4 cell culture. This cell line was formed by the electrofusion of a primary culture of human pancreatic islets with PANC-1, a human pancreatic ductal carcinoma cell line [31].

Anatomically, the pancreas consists of the islets of Langerhans, which are clusters of 5 different types of endocrine cells that secrete hormones into the blood. One of them is beta cells which uniquely synthesise, store, and release insulin - an anti-hyperglycemic hormone that antagonises glucagon, growth hormone, glucocorticosteroids, epinephrine, and other hyperglycemic hormones, to maintain circulating glucose concentrations within a narrow physiologic range.

Immunocytochemistry has shown that 1.1B4 cells secrete i.a. insulin, glucokinase, and IAPP (Islet amyloid polypeptide). They are also characterised by the expression of the glucose transporter GLUT1 [31].

1.1B4 cells were cultured in RPMI 1640 medium (Cat. No. 21875091) supplemented with 10% with Fetal Bovine Serum (Cat. No. 10500064), 2mM L-Glutamine (Cat. No. 25030081), 100 U/mL Penicillin and 100 mg/mL Streptomycin (Cat. No. 15140122). The cells were seeded into T75cm^2 flasks and grown at 37°C and 5% CO_2 under normoglycemic (NG) conditions.

Figure 5. 1.1B4 cell culture (left) and cells observed under the optical microscope at the confluence before passage, x10 magnification (right).

The dishes growing cells were observed daily under the microscope and passaged when they reached about 80% confluence as shown in Fig.5. For this purpose, after removing the medium, the cells were washed twice with PBS without Ca^{2+}, Mg^{2+} (cat. no. 10010015) and incubated with 0.25% trypsin - EDTA (Part No. 25200072) for about 10 minutes. When the cells detached from the dish surface, trypsin was inactivated by adding the medium with serum. The cell suspension was transferred to a tube and centrifuged at 260 × g for 10 minutes (g - acceleration due to gravity equal to 9.8 $\frac{m}{s^2}$). In the next step, the pellet was resuspended in fresh medium and the cells were counted using the Trypan Blue dye and the LUNA II automatic counter (20 µl of the dye and 20 µl of the cell suspension were pipetted and transferred to the counter plate). The cells were then seeded into new flasks (including hyper-flasks with an area of 600 cm^2) at an appropriate density. The total final culture area was 6 075 cm^2. Based on the measurement of the density of cells collected from a randomly selected dish with an area of 75 cm^2, the number of cells on a single dish was determined, which was 7.8 x 10^6 cells. All flasks were covered with cells to a similar extent (about 80% confluence), which was checked by the observation of the dishes with an optical microscope. Based on this data, the average number of cells per 1 cm^2 was calculated, which gave the result of 1.04 x 10^5 cells/cm^2.

3.2 Isolation and purification of extracellular vesicles

3.2.1 Differencial centrifugation

The first step in the isolation of EVs was to collect the medium from the 1.1B4 cell culture. Prior to this, all flasks were gently shaken to stimulate the cells to secrete more EVs. A total volume of 450 mL of the medium was divided into 50 mL falcon tubes and centrifuged for 10 minutes at 400 × g at 20°C for 10 minutes. The supernatant was then decanted and centrifuged for another 25 minutes at 3100 × g, also at 20°C. After that, the supernatant was once more centrifuged, at 7000 × g for 20 minutes (at 4°C). These steps make up the first stage of isolation, the purpose of which is to remove unwanted material from the sample, such as loosely suspended cells or their fragments and other larger impurities.

3.2.2 Low-pressure filtration

The next stage of isolation was low-pressure filtration with a dialysis membrane. The diagram and photo of the filtration system are shown in Fig.6.

The components of the system (according to the markings in Fig.6) are as follows:

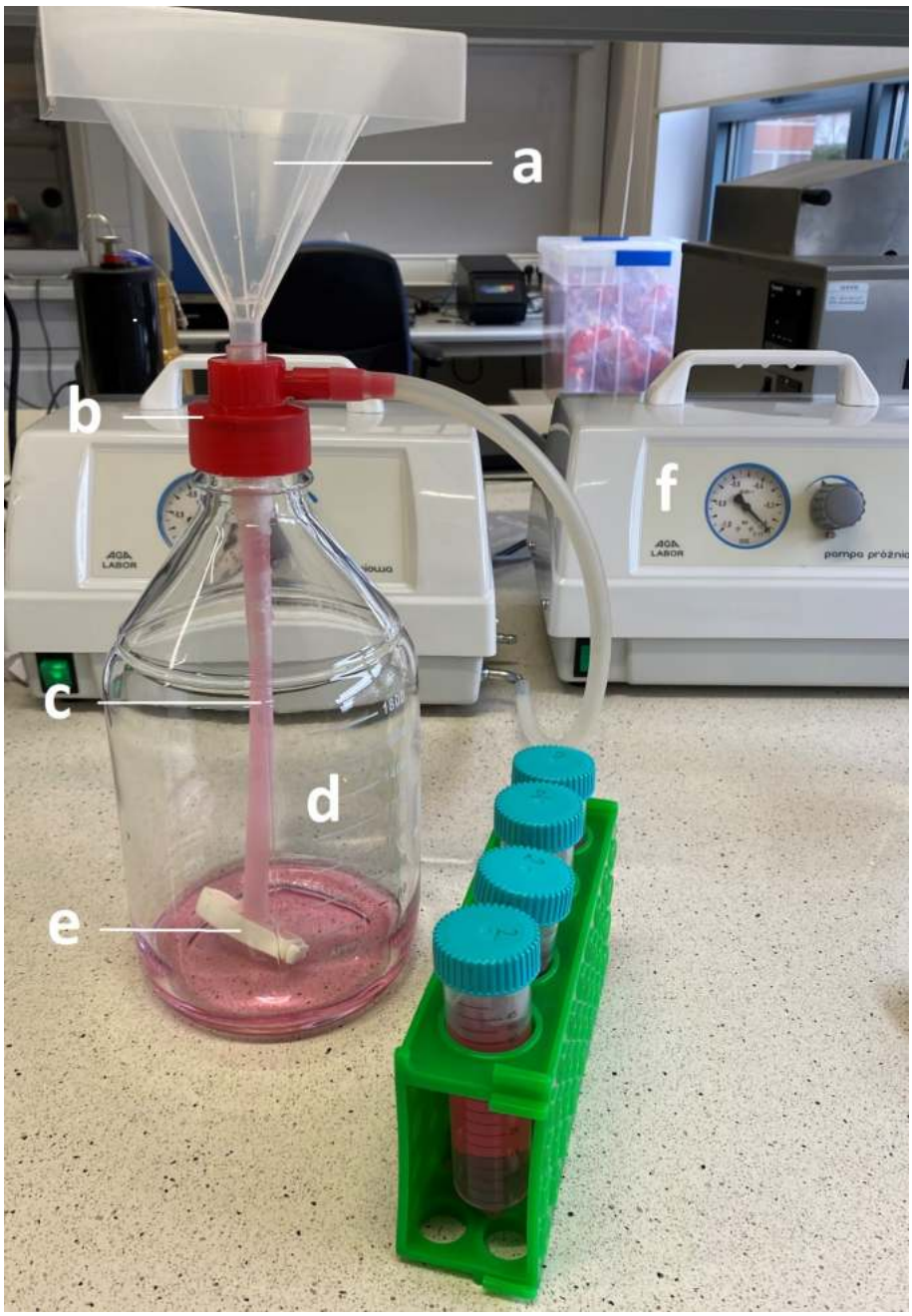

Figure 6. System used for EVs isolation with letter designations of individual elements.

(a) **closed liquid tank**, which allows maintaining sterile isolation conditions; its volume can be adjusted depending on the amount of sample

(b) **connector**, which is an intermediate element between the liquid reservoir and the rest of the system, most importantly the dialysis membrane

(c) **dialysis membrane**, on which isolated particles flowing down from the liquid tank located above are deposited; depending on the selection of the pore size of the membrane, particles of specific sizes are isolated

(d) **vacuum chamber**, which is also a storage tank for liquid filtered through the membrane

(e) **clamp**, closing the dialysis membrane at the bottom

(f) **pump**, which is a device that provides negative pressure in the system, which speeds up the isolation process and allows to limit the influence of time on changes in the sample.

After the initial set of centrifugations, the medium was placed in a liquid container and filtered through a dialysis membrane at a negative pressure of -0.3 bar. The filtration was performed on a dialysis membrane (cat. no. 131486, Spectra/Por Biotech) with a MWCO (molecular weight cutoff) of 1000 kDa. When a small amount of liquid (approx. 2 ml) remained at the end of the membrane, it was washed with 10-15 ml of deionized water to collect a clean sample of EVs (free of FBS, medium, or other contaminants).

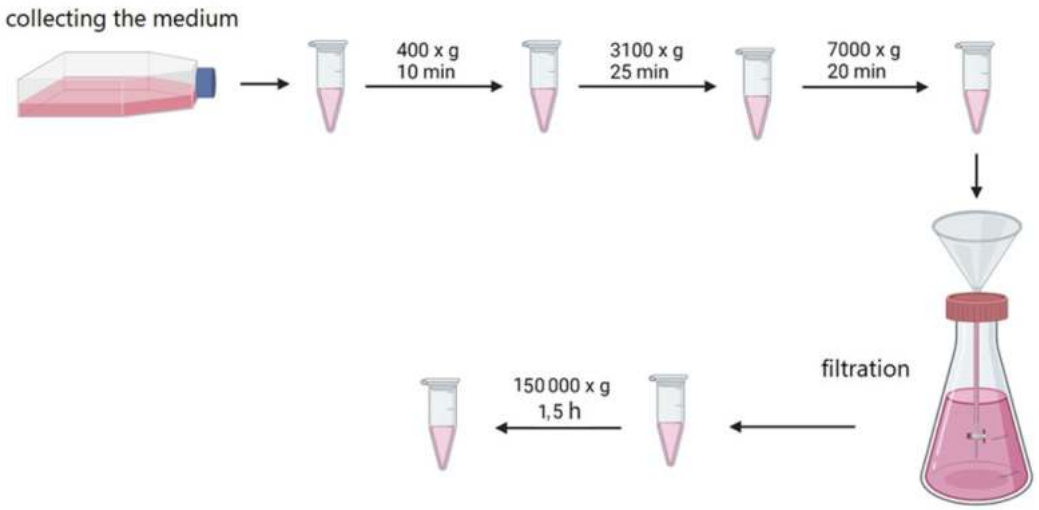

Figure 7. Diagram describing the preparation process for the EV sample.

3.2.3 Ultracentrifugation and the final sample

The final stage of sample preparation was ultracentrifugation at 150 000 × g for 90 minutes (at 4^{o}C). After this centrifugation supernatant was collected from EVs deposited at the bottom of the tube. This method of isolating EVs was developed in the research group of Prof. Stępień (Department of Medical Physics, Jagiellonian University, Krakow, Poland) and it has been thoroughly described in a number of publications [2][3][5][32]. About 1/4 of the vesicles isolated in this way were suspended in deionized water, as this part of the sample was intended for FTIR examination (10 µl). The rest (3/4) of the sediment was suspended in PBS, of which 10 µl) of the sample prepared in this way was used for measurement with the qNano device, and 210 µl) was left for the PALS measurement. The samples were stored at -80^{o}C until the analysis was initiated.

3.2.4 Environmental Scanning Electron Microscopy

Environmental Scanning Electron Microscopy (ESEM) measurements were performed to evaluate the diameter of pores in the dialysis membrane used for EVs isolation. A fragment of the dialysis membrane (approx. 1 x 0.5 cm) was placed on the sample holder and the subsequent ESEM measurements were performed using the SEM Quanta 3D FEG microscope (Fig.8). ESEM images were collected by a Low-Vacuum Secondary Electron Detector (LVED) using an electron beam of 20 keV energy. During the measurement, the specimen was kept at 130 Pa of water vapor at room temperature [33]. The measurements were performed by dr Konrad Szajna (Department of Solid State Physics, Jagiellonian University, Krakow, Poland).

Figure 8. EM Quanta 3D FEG microscope (FEI Company, Hillsboro, OR, USA), Department of Solid State Physics, Institute of Physics Jagiellonian University, Kraków, Poland (left); Dialysis membrane fragments placed on the SEM sample holder (right).

3.3 Tunable Resistive Pulse Sensing

Tunable Resistive Pulse Sensing (TRPS) is a nanoparticle analysis technique that involves the measurement of changes in electrical resistance as particles pass through a nanoscale pore, known as a nanopore, that is embedded in a thin membrane. It is a technique used for the characterization of various particles (such as EVs) based on their size, shape, and electrical properties.

TRPS typically involves a setup such as the qNano device, where a membrane with a pore of known size is placed between two chambers filled with an electrolyte solution.

After a precise calibration of the device (qNano, IZON), EVs suspended in PBS were injected into the upper chamber and electric potential and low pressure were applied across the nanopore. When particles pass through the pore, they cause temporary changes (pulses) in the electrical resistance, which can be measured as a current or voltage drop. The magnitude and duration of these changes in resistance are used to infer the size, shape, and concentration of the sample

Figure 9. IZON qNano device used to determine the concentration of the EV sample(left); An exemplary nanopore placed on a polyurethane membrane (right) [34].

contents. The size of a single resistive pulse is proportional to the volume of the particle, while the frequency of the pulses gives information about the concentration of particles in the sample.

3.4 Transmission Electron Microscopy

Transmission Electron Microscopy (TEM) is a powerful imaging technique used in materials science, biology, and other fields to obtain high-resolution images of the internal structure and ultrafine details of specimens at the nanometer scale. TEM uses a beam of electrons instead of light to image specimens, allowing for much higher magnification and resolution compared to optical microscopes [35].

A beam of electrons is generated in the TEM instrument and accelerated to high speeds using electromagnetic fields. The electron beam passes through a thin specimen causing interactions (such as scattering and diffraction) between the electrons and the specimen. The transmitted electrons are then collected by a detector, which generates an image that can be visualised on a screen or captured digitally.

In order to prepare the sample for the measurements using the TEM technique, the EV pellet was fixed with 2.5% glutaraldehyde solution (Cat. No. G5882) in 0.1 M cacodylic buffer (cat. no. C4945) for 2 h at room temperature. Subsequently, the sample was postfixed in 1% osmium tetroxide solution for 1 h, dehydrated by passing through graded ethanol series and embedded

in PolyBed 812 at 68^{o}C. Ultra-thin sections were collected on 300 mesh grids or one slot made from copper. The latter was additionally covered with formvar film. Leica EM UC7 microtome was used to cut the sections which were contrasted using uranyl acetate and lead citrate. The measurements were conducted using JEOL JEM 2100 H T electron microscope (Jeol Ltd, Tokyo, Japan) at an accelerating voltage of 80 kV. The measurements were performed by dr Olga Woźnicka (Department of Cell Biology and Imaging, Jagiellonian University, Krakow, Poland)

3.5 Fourier Transform Infrared Spectroscopy

Fourier Transform Infrared Spectroscopy (FTIR) is a technique used to analyze materials' chemical composition and molecular structure based on their infrared absorption and transmission properties. This tool is widely used in various scientific fields, including chemistry, materials science, biology, and pharmaceuticals [36].

In FTIR spectroscopy, a sample is exposed to a broad spectrum of IR radiation, typically ranging from mid-infrared to near-infrared wavelengths. The sample absorbs certain wavelengths of IR radiation, causing molecular vibrations and rotations that are characteristic of its chemical composition. The transmitted or reflected IR radiation is then measured, and a spectrum is obtained, which represents the unique fingerprint of the sample's molecular composition. The key component of FTIR spectroscopy is the Fourier transform interferometer, which is used to convert the interferogram (a measurement of the intensity of the IR radiation as a function of the optical path difference) into a spectrum. This allows for the simultaneous measurement of a wide range of IR wavelengths with high spectral resolution, providing detailed information about the chemical bonds, functional groups, and molecular structure of the sample.

Nicolet 6700 (ThermoFisher Scientific, MA, USA) spectrometer equipped with a diamond ATR attachment (Fig. 10) was used to investigate the EV sample. A measurement with the ATR (Attenuated Total Reflectance) attachment is a technique used to analyse the infrared spectrum of a sample without the need for extensive sample preparation. The ATR attachment allows for direct measurement of solid, liquid, and semi-solid samples by bringing them into contact with a crystal surface that acts as a waveguide for infrared light [32].

Firstly, the background measurement was performed and the device was properly calibrated. After these steps were performed, 5 µl of EV pellet suspended in deionized water was placed on the ATR crystal and left to dry (for approx. 30 minutes) in order to remove the signal coming from water in the resulting spectrum. The measurements were performed at room temperature and 256 scans were taken at a nominal resolution of 4 cm^{-1} using the mid-infrared spectrum range.

The measurements and analysis of the results were performed under the supervision and with

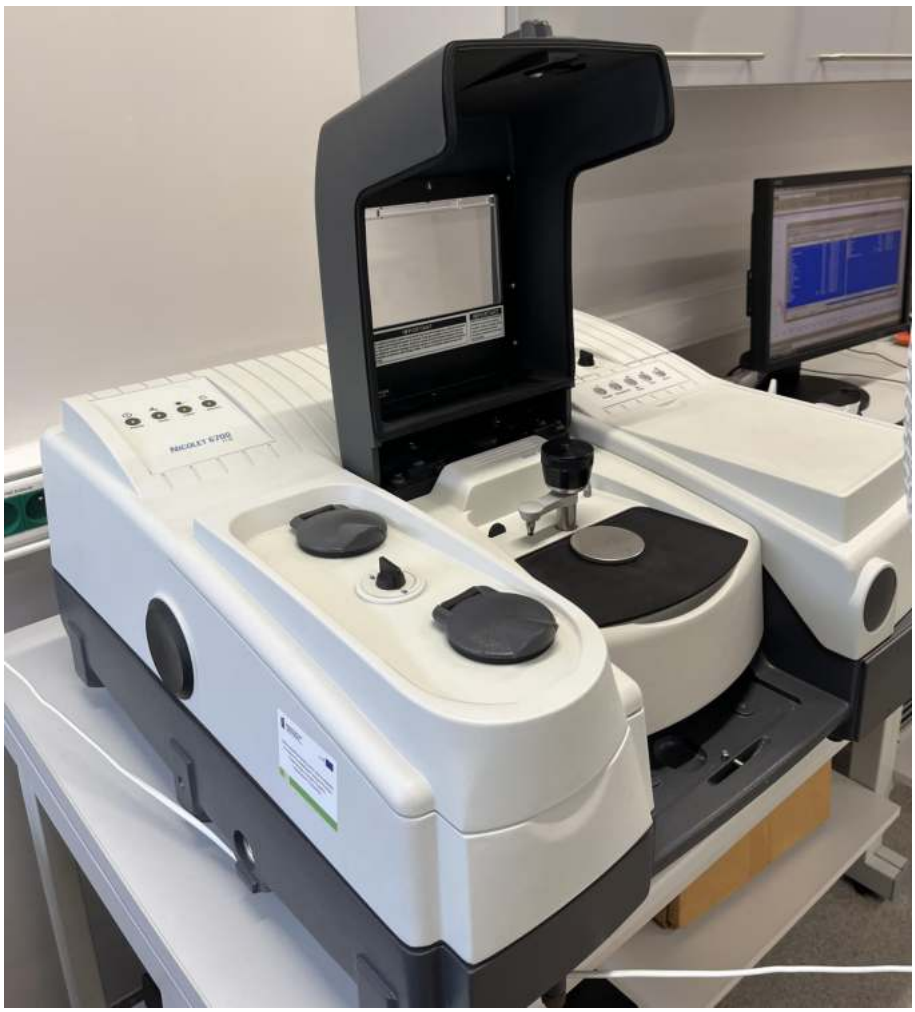

Figure 10. Nicolet 6700 (ThermoFisher Scientific, MA, USA) FTIR-ATR spectrometer, Department of Medical Physics, Institute of Physics Jagiellonian University, Kraków, Poland.

the help of Dr Andrzej Wróbel (Department of Medical Physics, Jagiellonian University, Krakow, Poland).

3.6 Positron Annihilation Lifetime Spectroscopy

PALS provides information on the size and distribution of voids or defects in materials. PALS measures the time it takes for positrons to annihilate with electrons in the material, which depends on the local environment. In this technique, a beam of positrons is directed into the sample being studied. They are typically implanted into the material and travel through the sample until they annihilate with electrons, producing gamma rays as a result of their mutual annihilation. The time delay between the implantation of the positrons and the detection of the resulting gamma rays is measured, and this time delay is referred to as the positron or positronium annihilation lifetime. In medical imaging such as PET, as much as 40% of positron annihilation occurs through the production of positronium atoms [37].

3.6.1 Source of positrons

Sodium-22 isotope in the form of a ^{22}NaCl solution sealed between two sheets of 6 µm thick Kapton film was used as a source of positrons. In order to conduct safe measurements with liquid samples (without the risk of isotope leakage through the Kapton), the source was additionally wrapped in a thin layer of Parafilm®M. ^{22}Na has a half-life of 2.6 years and decays via β^+ decay to excited state neon-22 with simultaneous emission of a positron and an electron neutrino. This isotope is commonly used in various scientific and medical applications, including PET and PALS. It is so because, in addition to the positron, it also emits a gamma quantum with an energy of 1274 keV, i.e. a deexcitation quantum (Fig. 11), according to the reaction chain:

$$^{22}_{11}Na \rightarrow {}^{22}_{10}Ne^{*} + \ e^{+} + \nu_e \rightarrow {}^{22}_{10}Ne + \gamma + \ e^{+} + \nu_e \ . \tag{3}$$

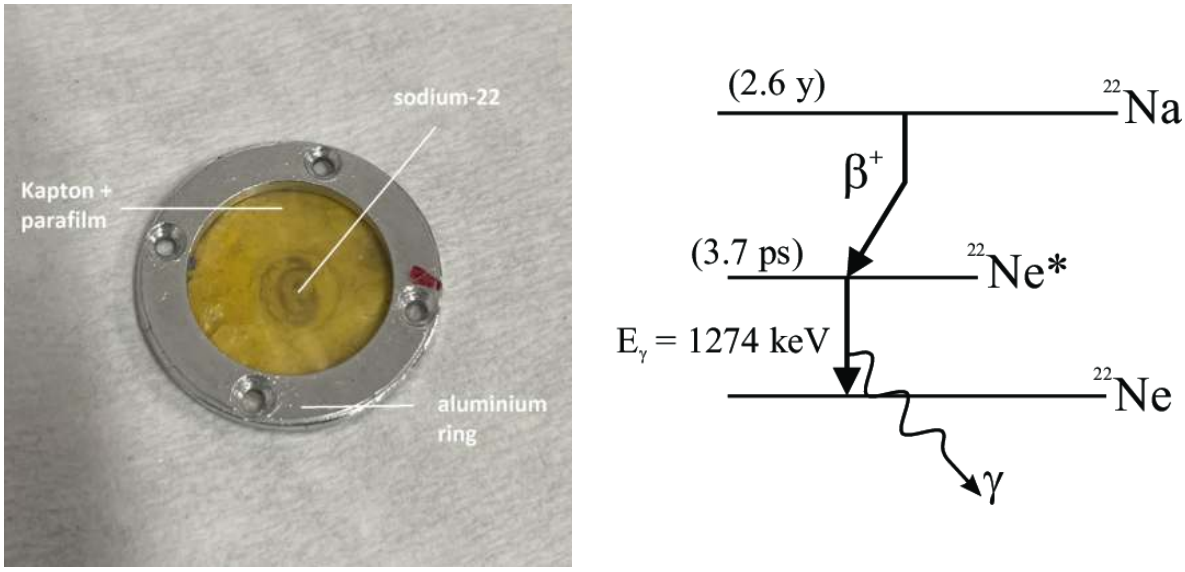

Figure 11. ^{22}Na source in Kapton foil and protective Parafilm layer attached to a metal ring designed for mounting in the measuring chamber (left); Simplified decay scheme of ^{22}Na [38] (right).

Gamma quanta, originating from the deexcitation of $^{22}_{10}Ne^{*}$, are emitted 3.7 ps (on average) after the emission of a positron [39]. Since the emission of the 1274 keV gamma quantum occurs almost simultaneously with the production of the positron, this time is considered to be the beginning of positronium formation.

The sodium source used for this PALS study (source No. 2/2021) on the day of production (2021 March 25) had an activity of 1.3 MBq. On measurement days (Beta cells: 2022 March 10, EVs: 2022 June 15, PBS: 2022 July 4) its activity was approximately 1, 0.9, and 0.9 MBq respectively.

3.6.2 PALS setup

Figure 12 presents a scheme of the setup used to investigate EVs in terms of the positronium lifetime. It slightly differs from standard PALS systems, as it was appropriately adapted to allow studies with biological material.

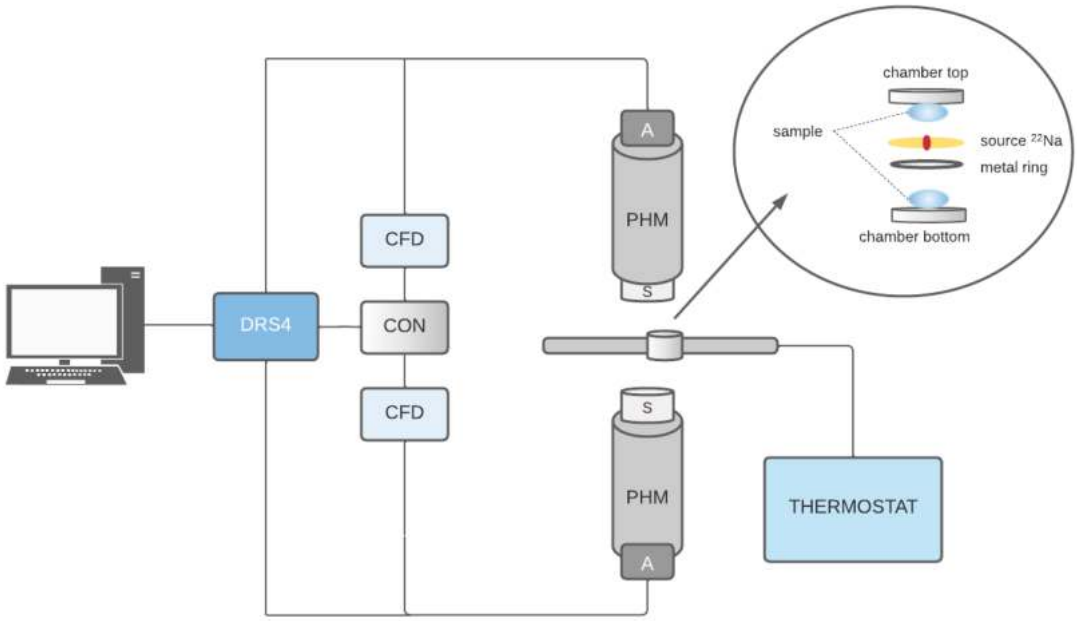

Figure 12. Diagram of the PALS system with marked individual elements, where: PHM - photomultiplier, A - attenuator, CFD - constant fraction discriminator, CON - coincidence module, and DRS4 is an evaluation board.

Its main components are two H3378-51 Hammamatsu photomultipliers (PHM) together with two Scionix cylindrical scintillators BaF_2 (S) with a diameter of 38 mm and a height of 25 mm. The system is powered by CAEN SY4527 high-voltage power supply. The signals from the photomultipliers were attenuated (A) and delivered to the LeCroy 608C constant fraction discriminator (CFD), where appropriate thresholds were set for signals from different detectors. A high threshold (-90 mV) was used on the first detector to register only the deexcitation gamma quantum with the energy of 1274 keV (START signal). On the second detector, the low threshold (-27 mV) allowed to register the annihilation quantum with the energy of 511 keV (STOP signal). On the LeCroy 622 coincidence module (CON) a coincidence time window of 110 ns was set. Data from the measurements was collected via the DRS4 evaluation board. During the measurement, the source was displaced relative to the axis of the center between the detectors by a distance greater than the radius of the scintillator. This made it geometrically impossible to register annihilation quanta by both detectors and allowed to register only pairs of deexcitation and annihilation gamma quanta. The system was also equipped with the Lauda LOOP L100 thermostat, which allows controlling the sample temperature in the range of 4-80°C with an accuracy of 0.1°C. The exact

setup on which the research for this thesis was carried out and the measuring chamber are shown in Figures 13 and 14.

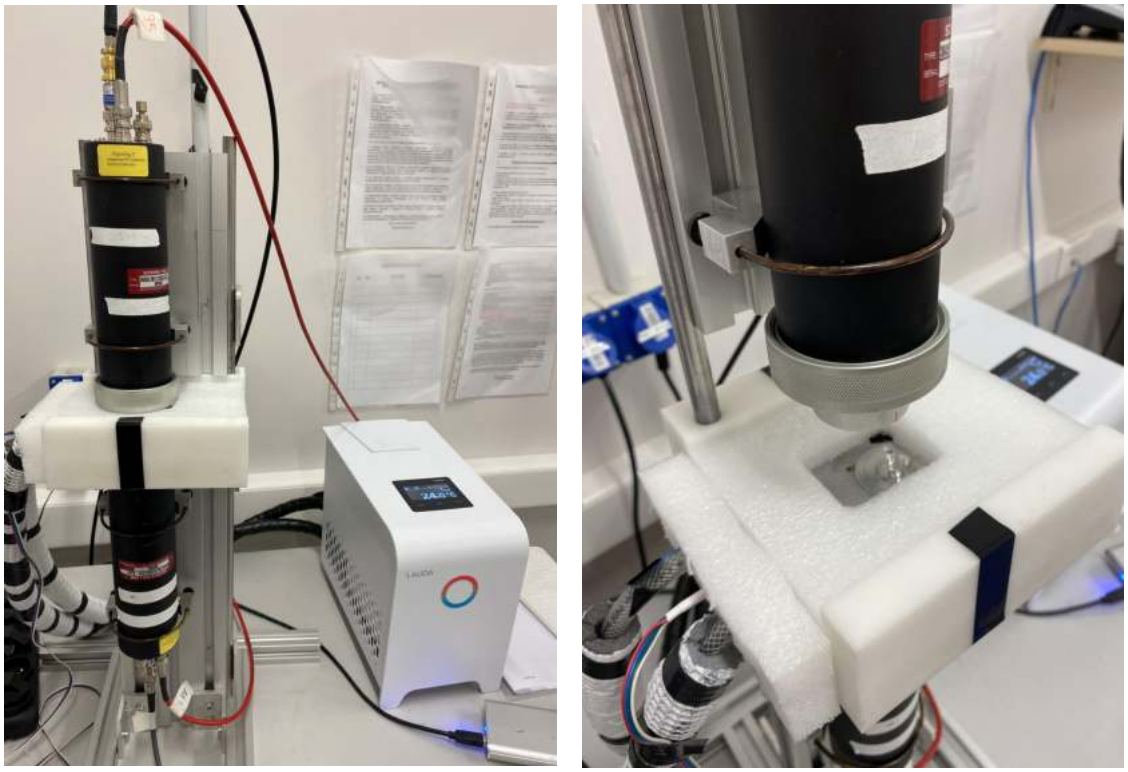

Figure 13. PALS setup, Department of Experimental Particle Physics and Applications, Institute of Physics Jagiellonian University, Kraków, Poland.

Figure 14. Measuring chamber; it was specially designed so that it is possible to perform measurements even with a small amount of sample. It is spherical in shape with a radius of 7mm and has a total volume of 200 μm (100 μm at the bottom and 100 μm at the top part).

3.6.3 Signal analysis

The first step of signal registration was the conversion of the gamma quantum into a light signal by scintillators. Then, photomultipliers converted the photons from the scintillators into an electrical signal that is a voltage-time dependence on a given channel of the oscilloscope. Using a specially developed program ”Read Binary” (K. Dulski, J-PET collaboration) [40], the deposited

charge and signal amplitude were calculated on the basis of a single signal. These quantities were necessary to distinguish gamma annihilation and deexcitation quanta, as well as to determine the time difference between signals coming from two photomultipliers, and thus the positronium lifetime.

The signals were sampled at discrete points as shown in Figure 15. The signal pedestal was calculated as the average value of 10 points, leaving out the first 20 points from the left of the spectrum. The amplitude was calculated as the minimum value of the signal.

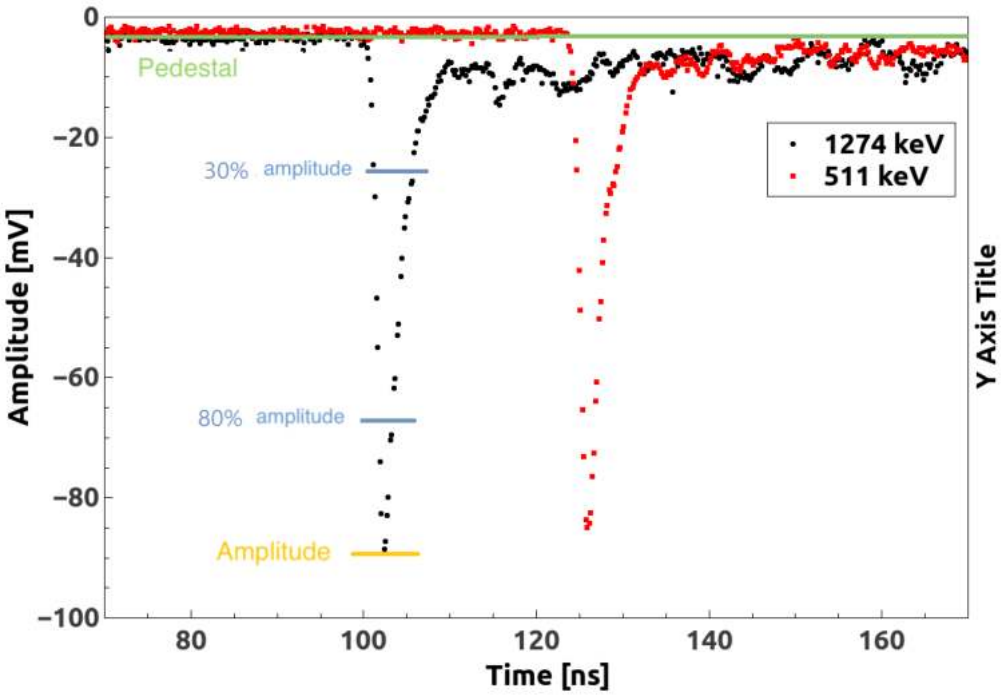

Figure 15. An exemplary pair of signals from both detectors. The green color shows the pedestal of the signal, the yellow line indicates the signal amplitude and the blue lines indicate the signal height at 30% and 80% of the amplitude.

To estimate the time at a given voltage, a linear function was fitted to the edge of the signal in the range of 30% to 80% of the amplitude. The time (t) was determined by the intersection of the fitted line with the voltage level corresponding to 10% of the amplitude. The area under the signal determined the value of the deposited charge according to the equation:

$$Q = \int \frac{U(t)dt}{R}, \tag{4}$$

where U(t) is the signal voltage and R is the resistance of a given channel on the DRS4 board, which had a constant value of 50 Ω for all measurements. Different trigger thresholds were used to increase the statistics in the right area. For the detector assigned to recording the gamma deexcitation quantum, the threshold was -90 mV, and for the detector assigned to recording the

gamma annihilation quantum, the threshold was set to -27 mV.

The lifetime of positronium was determined using the "PALSavalanche" program (K. Dulski, J-PET collaboration). The experimental distribution of the positronium lifetime spectrum for a single component (τ) can be approximated by the function:

$$F(t;\tau,t_0,\sigma) = \frac{1}{2\tau} exp\Big(\frac{\sigma^2}{2\tau^2} - \frac{t-t_0}{\tau}\Big)\Big(erf\Big(\frac{t-t_0-\frac{\sigma^2}{\tau}}{\sqrt{2}\sigma}\Big) - erf\Big(\frac{-t_0-\frac{\sigma^2}{\tau}}{\sqrt{2}\sigma}\Big)\Big), \tag{5}$$

where t_0 – detector time offset, σ - instrument resolution, t - time difference between detectors, τ - average positronium lifetime, and erf is the error function defined as [40]:

$$erf(t) = \frac{2}{\sqrt{\pi}} \int_0^x exp(-s^2)\ ds. \tag{6}$$

Four basic components ($n_\tau = 4$) corresponding to lifetime and intensity were matched to the spectrum:

τ_1, I_1 - para-positronium annihilation

τ_2, I_2 - free positrons annihilation

τ_s, I_s - positron annihilation in the source material (Kapton foil)

τ_3, I_3 - ortho-positronium annihilation.

In order to determine the distribution of the mean positronium lifetime, one must assume a discrete distribution of free volumes and thus a discrete contribution of individual components with an average lifetime. The following function is fitted [40]:

$$f(t) = y_0 + \sum_{i=1}^{n_\tau} I_i \cdot F(t;\tau_i;t_0;\sigma), \tag{7}$$

where y_0 - background level, n_τ - number of components, I_i - intensity of i-th component, τ_i - mean lifetime of i-th component, and $F(t;\tau_i,t_0,\sigma)$ is a function expressed by the equation (5).

The lifetime and intensity of the annihilation component in the source material (τ_s, I_s) and the p-Ps lifetime were determined beforehand and fixed in the analysis. The corresponding values were 0.374 ns, 10% and 0.125 ns, respectively [24]. All other components were treated as free parameters in the fitting equation (7). Figure 16 shows an exemplary positronium lifetime spectrum with fitting of appropriate functions.

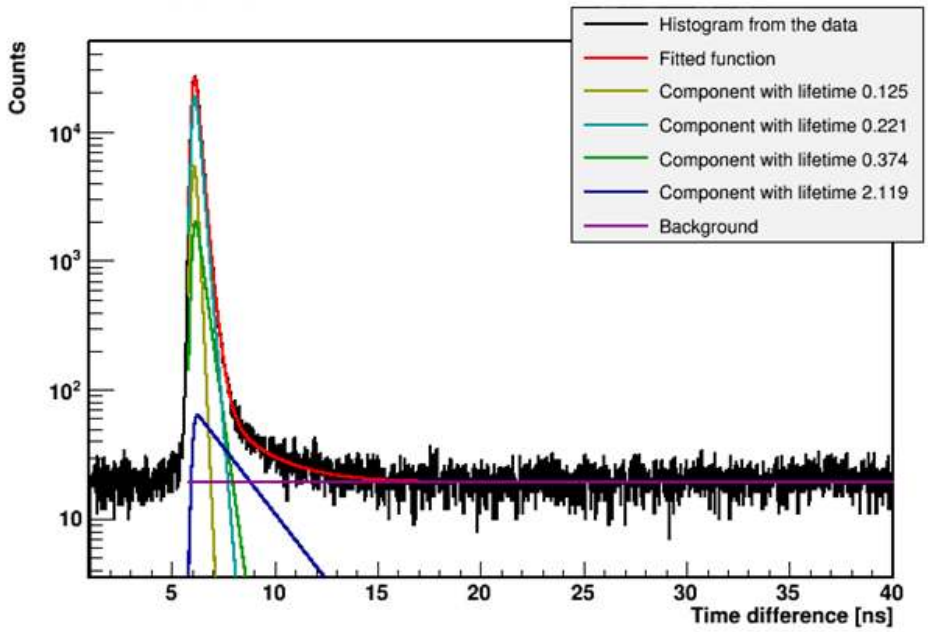

Figure 16. An exemplary spectrum of the positronium lifetime in the extended scale. The superimposed lines indicate the resulting distributions of individual components from the fitting equation (7). Red indicates the fitted function, green - the distribution of p-Ps, yellow - annihilations in the source material, turquoise - annihilations of free positrons in the sample, blue - annihilations of o-Ps, and purple - the background level.

4. Results

4.1 ESEM: dialysis membrane pore diameter

ESEM was used to visualize pores in the dialysis membrane. Figure 17 shows exemplary images obtained with ESEM. These measurements revealed the irregular structure of the membrane with pores varying in diameter from approx. 20 nm to 60 nm. The average pore size calculated from the 50 randomly selected pores was 36 ± 11 nm.

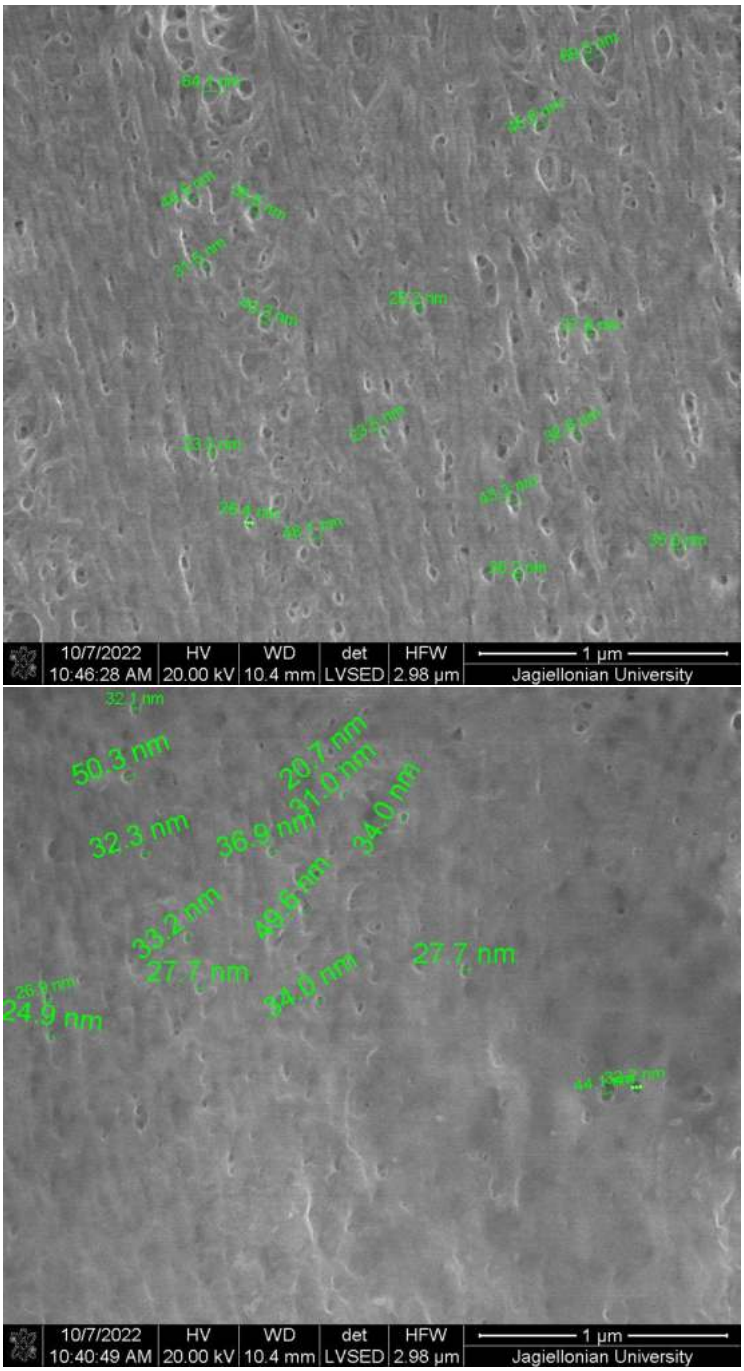

Figure 17. Exemplary ESEM images of the dialysis membrane surface, with the sizes of several pores indicated.

4.2 TRPS: EV concentration and size distribution in the sample

EV concentration in the sample after isolation was measured using the qNano device [16]. Figure 18 shows the obtained results. The mean concentration of EVs in the samples after ultracentrifugation and suspension in PBS was 7,82E+11 particles/ml. This result allowed to estimate the average number of vesicles released from 1 cm^2 of the cell culture area. Considering that the total area of the culture was 6075 cm^2, the result of such calculations gives 2.83E+07 EVs/cm^2. Based on this data, the number of EVs secreted by a single cell in the culture was also estimated and the result was 2.72E+02 EVs/cell.

The average size of the EVs detected was 207 nm. Vesicles with a diameter lower than 100 nm were not detected.

4.3 TEM: EV visualization and size distribution

TEM was used to confirm the presence of EVs in the prepared sample. Figure 19 shows representative images of the isolated EVs. Especially large vesicles with a diameter of approx. 300-400 nm are clearly visible. In some cases, we can even distinguish the membrane of the vesicle and distinct granules inside it. Using the ImageJ program, the average EV diameter was determined to be 216 nm (based on 25 randomly selected vesicles visible in TEM images.

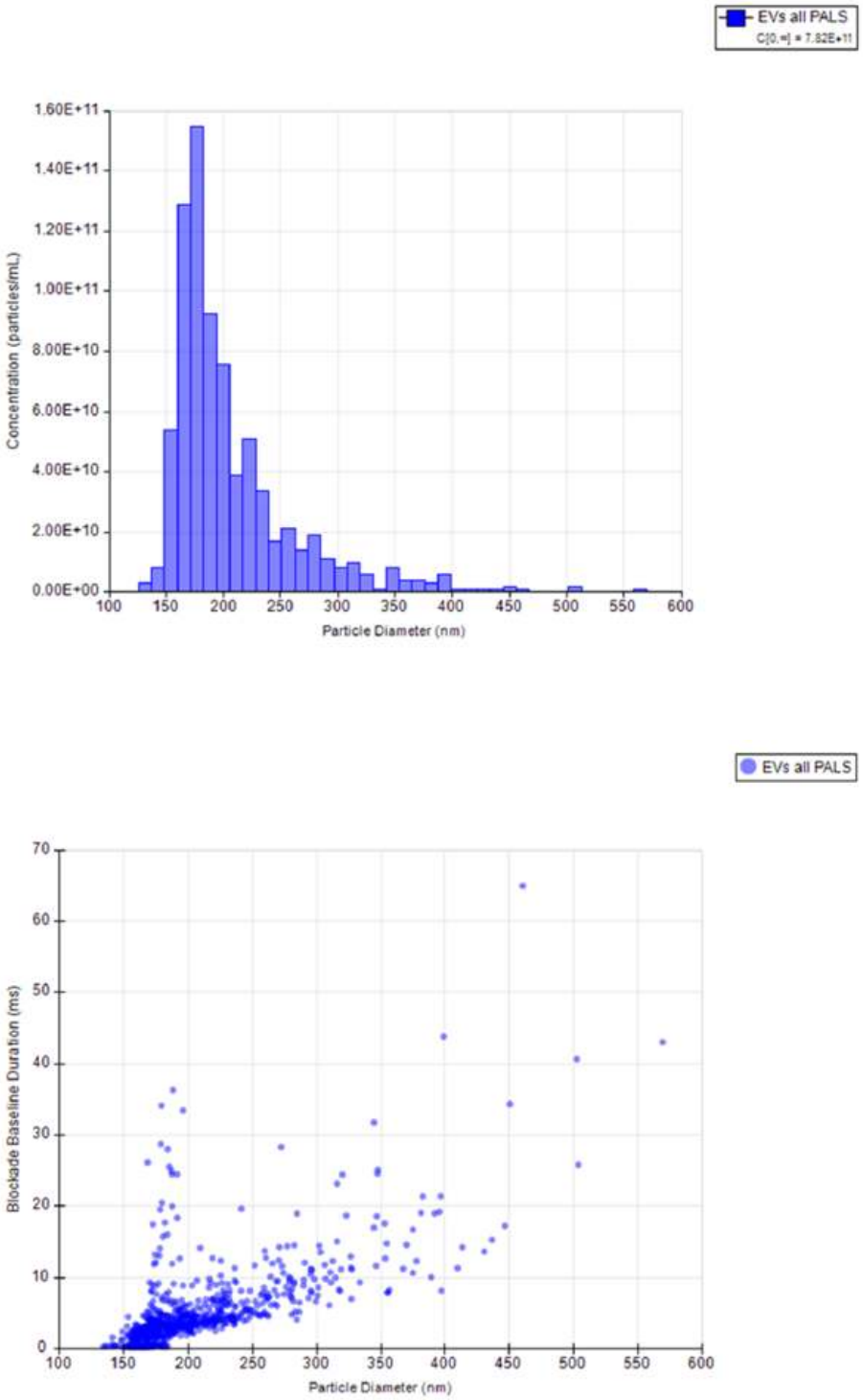

Figure 18. Results of the TRPS measurement with qNano device.

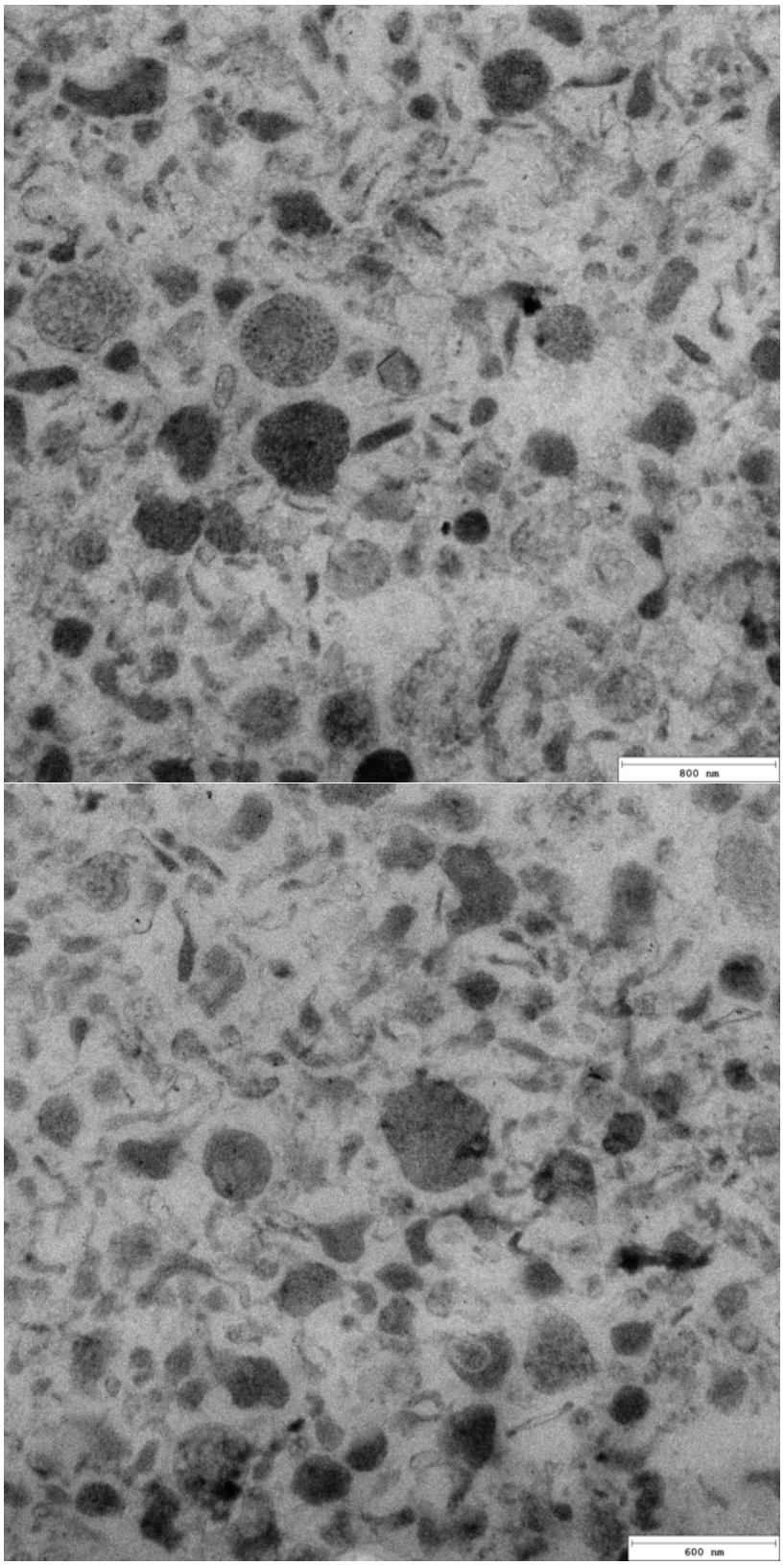

Figure 19. Representative TEM images of isolated EVs.

4.4 FTIR: infrared spectra of EVs

ATR-FTIR spectrum obtained for the EV sample is presented in Figure 20. The FTIR spectrum in the mid-infrared range consists primarily of lipid and amid components. In the amide component, Amid I (1650 cm^{-1} originating mainly from C=O vibrations of the protein-peptide backbone) and Amid II (1540 cm^{-1}, originating from N–H vibrations of the peptide groups) bands can be distinguished [32].

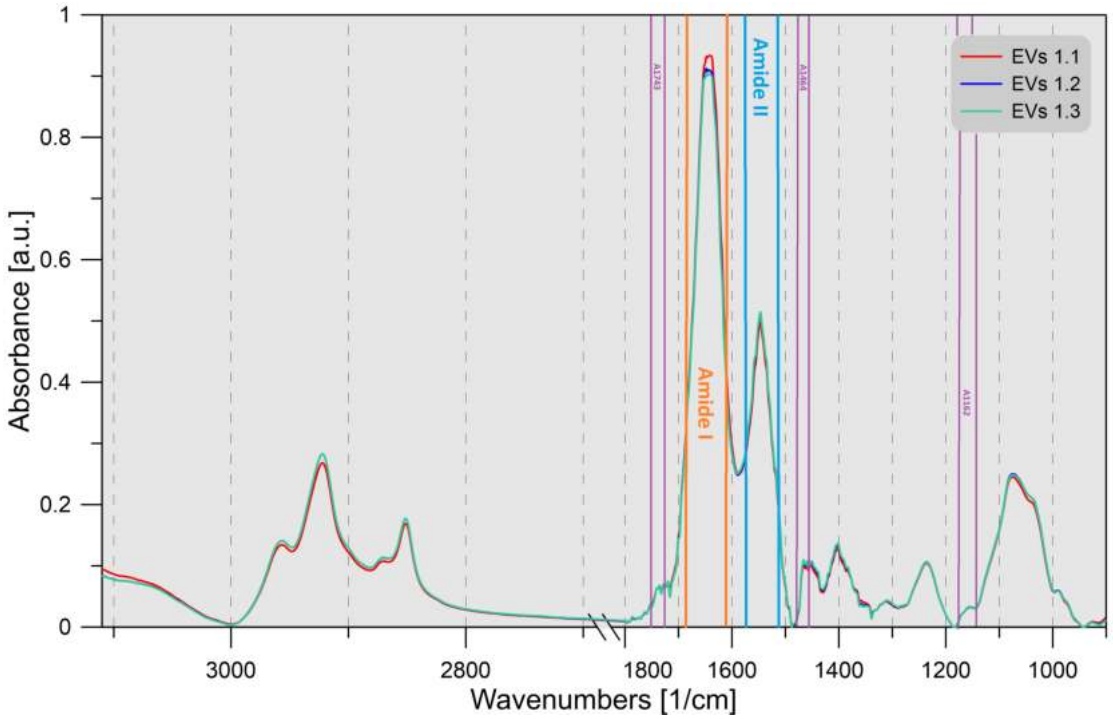

Figure 20. The average ATR-FTIR spectrum of EVs derived from 1.1B4 cell line culture with marked bands corresponding to proteins (amide I and amide II) and lipids (A1162, A1464, A1743).

4.5 PALS measurements

4.5.1 PBS

The aim of one of the measurements using the PALS instrument was to examine the lifetime and intensity of o-Ps in the PBS buffer in which the EVs from the main sample were suspended (Table 2). Measurements were made at 22°C and 34.2°C. The duration of a single measurement was about 60 minutes (for the statistics of 1 million events). The presented measurement uncertainties are the standard deviation for the average of three measurements. The lifetime and intensity of the annihilation component in the source material (τ_s, I_s), as well as the lifetime of p-Ps (τ_1), were fixed in the analysis. Their values are τ_s = 0.374 ns, I_s = 10%, and τ_1 = 0.125 ns respectively. In addition, the τ_p and I_p components derived from the annihilation in the parafilm were assumed as

Table 2. Results of Positron Annihilation Lifetime Spectroscopy for the PBS buffer.

Temperature (°C)	22		34,2	
	Lifetime [ns]	Intensity [%]	Lifetime [ns]	Intensity [%]
Para-Positronium	0,125	17.3	0,125	18,2
		17,8		18,1
		18,4		19,6
Mean value	0,125	17,8(6)	0,125	18,6(8)
Free positrons	0,391	54,8	0,392	54,2
	0,390	54.0	0,389	54.1
	0,394	53.9	0,394	53,0
Mean value	0,392(002)	54,2(5)	0,391(003)	53,8(6)
Ortho-Positronium	1,82	14,8	1,78	14,4
	1,79	15,0	1,77	14,6
	1,82	14,6	1,79	14,2
Mean value	1,81(02)	14,8(2)	1,78(01)	14,4(2)

constant values (based on designated measurements with parafilm). They were respectively 2.35 ns and 3.1% at 22°C and 2.62 ns and 3.2% at 34.2°C. The o-Ps results from Table 2 are also shown in Figure 21. Exemplary measurement spectra for PBS are shown in Figure 22.

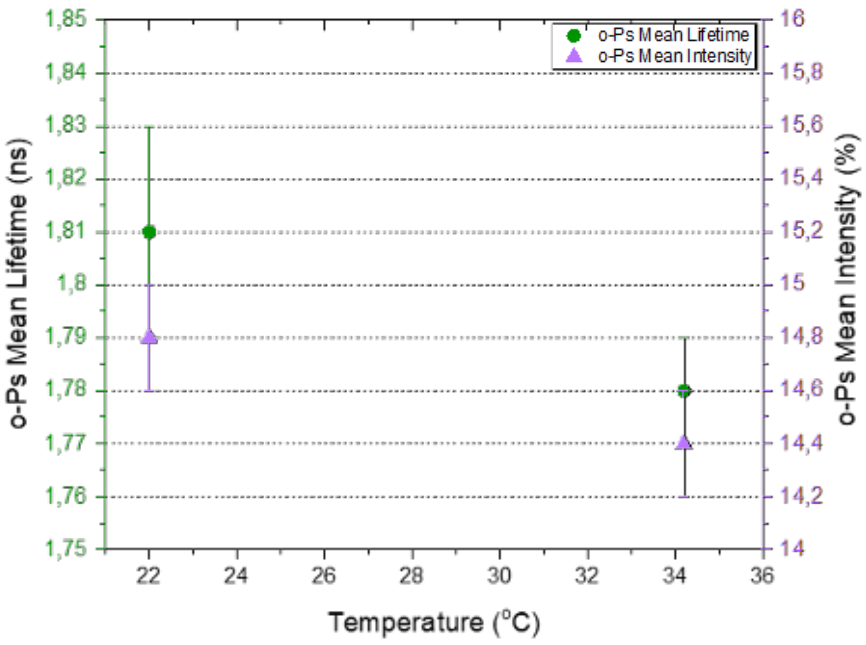

Figure 21. Graphic representation of o-Ps lifetime and intensity results for the PBS buffer.

4.5.2 Pancreatic beta cells

In an additional series of measurements, cells of the 1.1B4 line, from which EVs were isolated, were also examined. Measurements were carried out at 22°C and 34.2°C on both cells stored at -80°C and cells harvested straight from the culture. Viability tests showed the viability of 44.8%

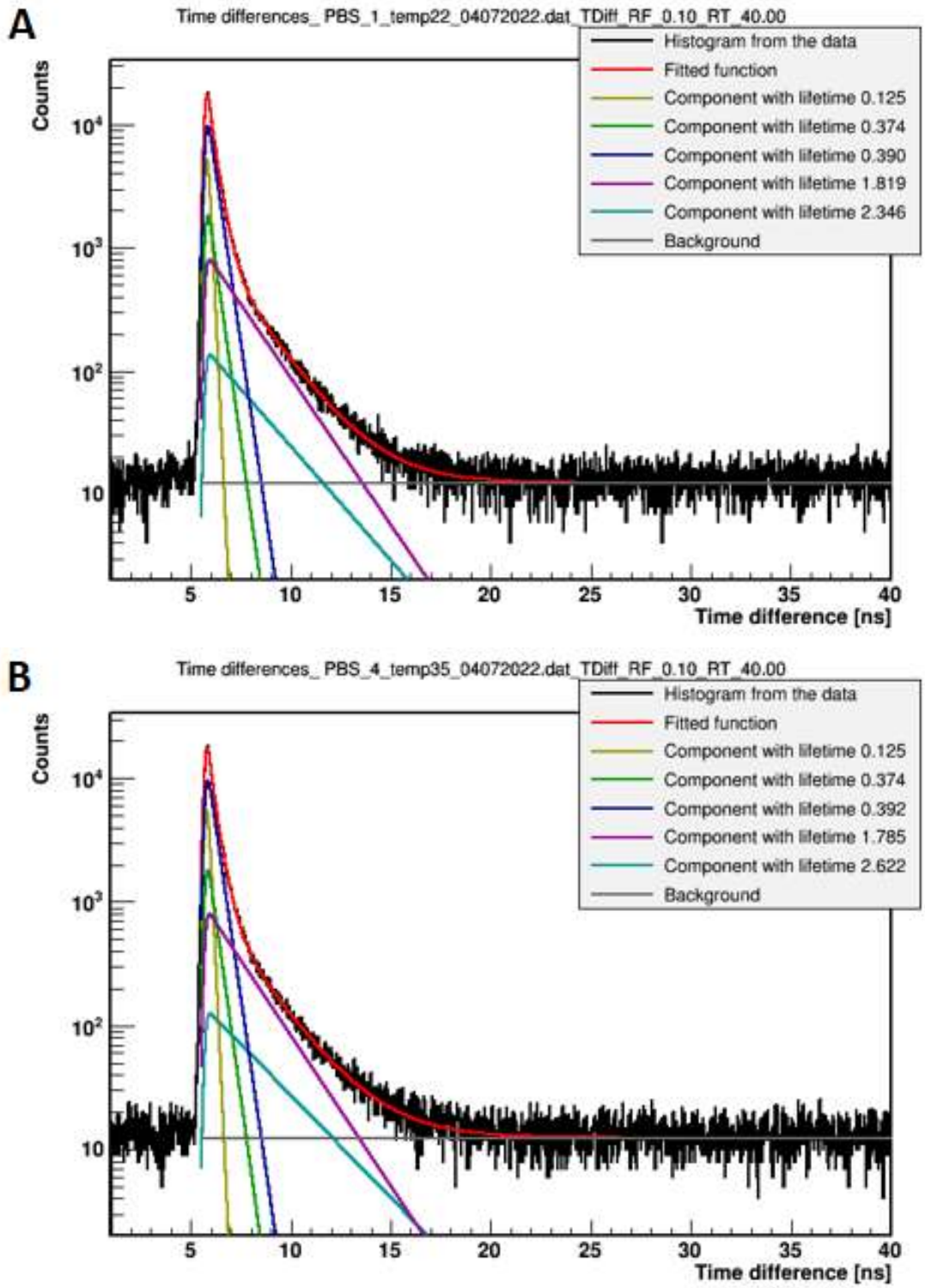

Figure 22. An exemplary spectra of the positronium lifetime in the PBS buffer measured at 22°C (A) and 34.2°C (B) - the extended scale. The superimposed lines indicate the resulting distributions of individual components from the fitting equation (7). Red indicates the fitted function, yellow - the distribution of p-Ps, green - annihilations in the source material (Kapton), turquoise - annihilations in the parafilm, dark blue - annihilations of free positrons in the sample, purple - annihilations of o-Ps, and grey - the background level.

Table 3. Results of Positron Annihilation Lifetime Spectroscopy for the beta-pancreatic cells stored at -80°C and thawed (1), and cells harvested straight from the cell culture (2).

Temperature (°C)	22	34.2	22	34.2
Sample	1.Thawed		2.Alive	
O-Ps mean lifetime (ns)	1,963	1,948	1,908	1,909
Error	0,030	0,010	0,041	0,059
O-Ps intensity (%)	16,4	16,5	15,5	16,0
Error	0,4	0,8	0,2	0,2

Temperature (°C)	22	34.2	22	34.2
Sample	1.Thawed		2.Alive	
Free positrons mean lifetime (ns)	0,396	0,405	0,387	0,395
Error	0,007	0,003	0,005	0,021
Free positrons intensity (%)	58,7	58,3	56,7	57,0
Error	0,5	0,1	1,2	0,1

and 97.1%, respectively. In both cases, the 200 μl chamber was fully filled with a cell pellet. As before, the lifetime and intensity of the annihilation component in the source material and the lifetime of p-Ps were fixed in the analysis. The intensity of the p-Ps annihilation component was approximately 20% in each measurement. The results of these measurements are presented in Table 3, and the exemplary spectra obtained from the measurements of both types of cells performed at 22°C are shown in Figures 23 and 24.

4.5.3 EVs

For the EVs sample, measurements were performed at T = 22°C and T = 34.2°C (three repetitions, without dismounting the chamber). The results for EVs are shown in Table 4. The lifetime and intensity of the annihilation component in the source material, the lifetime of p-Ps, and the annihilation components in the parafilm were fixed in the analysis, identically to the measurements of PBS and beta cells. The results from EVs measurements are presented in the table 4. Figure 26 shows exemplary spectra obtained from the measurements at 22°C and 34.2°C. Without opening the measurement chamber, after the third measurement at 34.2°C, a single additional measurement at 22°C was performed. The o-Ps lifetime obtained in this measurement was 1.90 ns, and its intensity was 15.2%.

Figure 25 shows a graphical representation of the results for EVs, while Figure 27 shows a comparison of the results for EVs and PBS in which the vesicles were suspended.

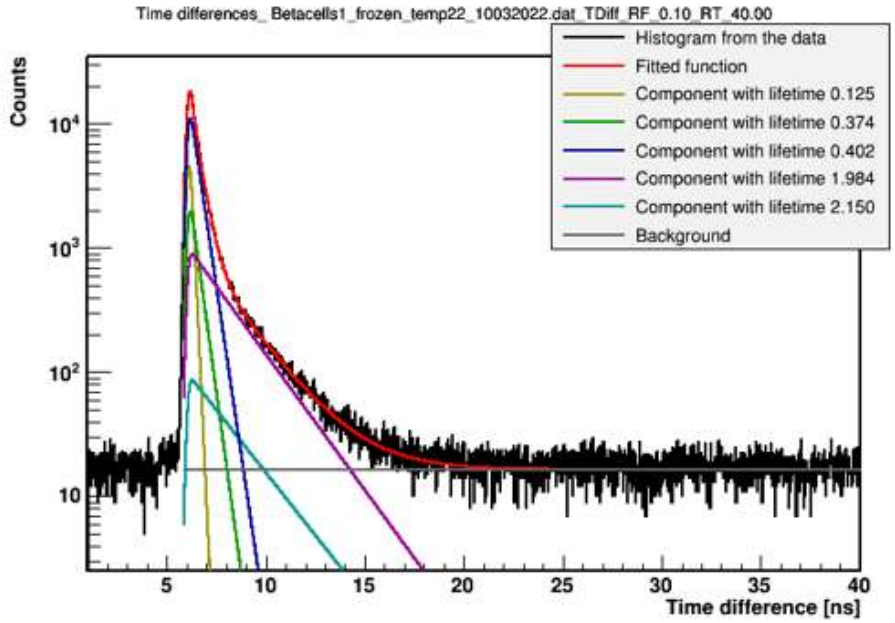

Figure 23. An exemplary spectra of the positronium lifetime in thawed beta-pancreatic cell pellet measured at 22°C - the extended scale. The superimposed lines indicate the resulting distributions of individual components from the fitting equation (7). Red indicates the fitted function, yellow - the distribution of p-Ps, green - annihilations in the source material (Kapton), turquoise - annihilations in the parafilm, dark blue - annihilations of free positrons in the sample, purple - annihilations of o-Ps, and grey - the background level.

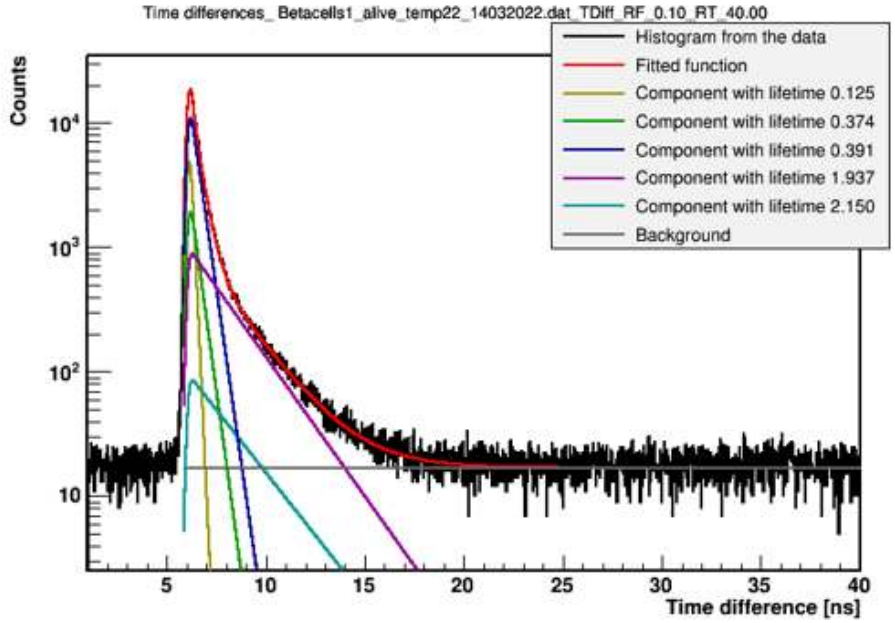

Figure 24. An exemplary spectra of the positronium lifetime in beta-pancreatic cell pellet harvested straight from the cell culture measured at 22°C - the extended scale. The superimposed lines indicate the resulting distributions of individual components from the fitting equation (7). Red indicates the fitted function, yellow - the distribution of p-Ps, green - annihilations in the source material (Kapton), turquoise - annihilations in the parafilm, dark blue - annihilations of free positrons in the sample, purple - annihilations of o-Ps, and grey - the background level.

Table 4. Results of Positron Annihilation Lifetime Spectroscopy for the EV sample.

Temperature (°C)	22		34,2	
	Lifetime [ns]	Intensity [%]	Lifetime [ns]	Intensity [%]
Para-Positronium	0,125	16,6	0,125	17,8
		16,4		18,1
		16,1		17,3
Mean value	0,125	1 6,4(2)	0,125	17,7(4)
Free positrons	0,403	54,9	0,409	54,0
	0,405	55,3	0,409	53,8
	0,401	55,3	0,402	54,3
Mean value	0,403(002)	55,2(3)	0,407(004)	54,0(3)
Ortho-Positronium	1,89	15,4	1,84	15,0
	1,87	15,2	1,84	14,9
	1,86	15,4	1,81	15,2
Mean value	1,87(02)	15,4(2)	1,83(02)	15,0(1)

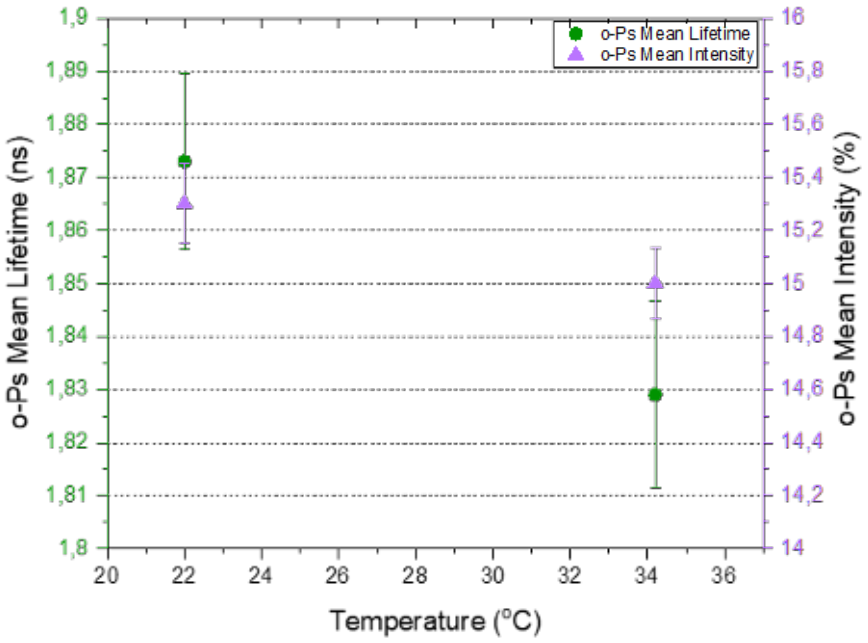

Figure 25. Graphic representation of o-Ps lifetime and intensity results for the EV sample.

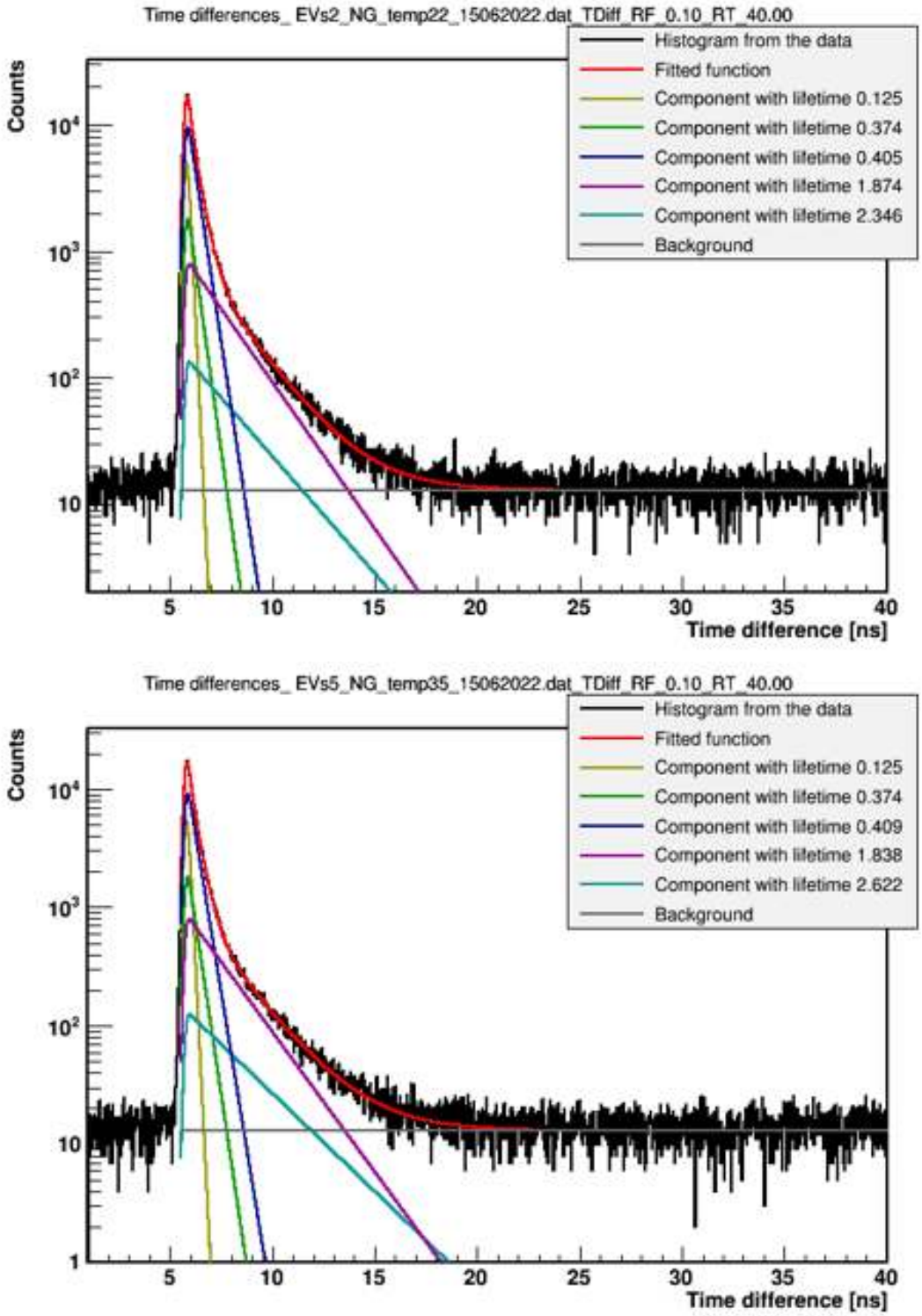

Figure 26. An exemplary spectra of the positronium lifetime in the EV sample measured at 22°C (A) and 34.2°C (B) - the extended scale. The superimposed lines indicate the resulting distributions of individual components from the fitting equation (7). Red indicates the fitted function, yellow - the distribution of p-Ps, green - annihilations in the source material (Kapton), turquoise - annihilations in the parafilm, dark blue - annihilations of free positrons in the sample, purple - annihilations of o-Ps, and grey - the background level.

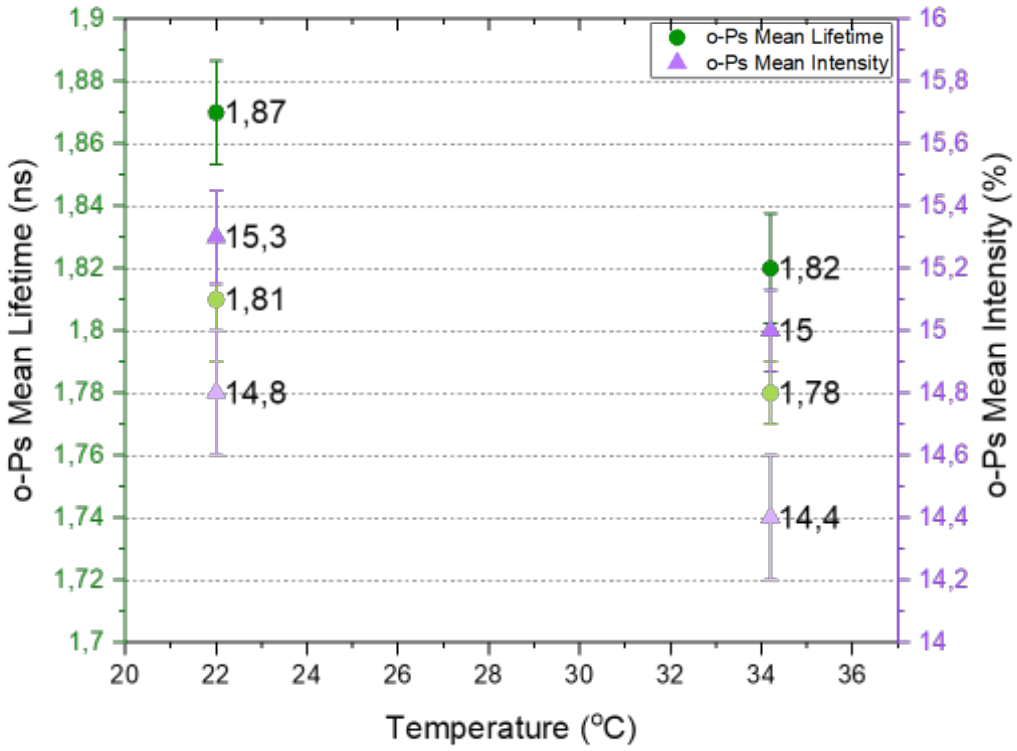

Figure 27. Comparison of o-Ps lifetime and intensity results for EVs (dark green and purple, respectively) and PBS buffer (light green and purple, respectively).

5. Discussion

The aim of this thesis was to propose a methodology for determining the mean o-Ps lifetime in a sample of EVs derived from cell culture.

The vesicles were isolated from a 2D large-scale culture of human pancreatic beta cells maintained under normoglycemic conditions. Isolation was performed by low-pressure filtration. Using the ESEM technique, images of the dialysis membrane were obtained, which showed that the membrane pores are smaller (<100 nm) in comparison to the size of EVs (>100 nm). This result suggests that most of the isolated EVs would remain on the membrane allowing the sample to be collected for ultracentrifugation.

The data obtained from measurements based on TRPS technology (qNano device) provided insights into the vesicle population, including their average size and heterogeneity. The results showed that in the obtained sample, vesicles with a diameter between 150 and 250 nm were the most abundant. Therefore, based on Table 1, isolated EVs can be classified as microvesicles. This method also allowed to determine the concentration of vesicles in the sample, which was 7,82E+11 particles/ml. It is a considerable concentration for vesicles obtained from a traditional 2D cell culture, and the large scale of the culture contributed to this result. It has also been previously shown that higher concentrations of EVs may be obtained under specific stimuli (e.g. stress or mechanical stimulation) such as performed here cell starving and flask shaking.

The TEM technique provided high-resolution images of EVs and allowed for the morphological characteristics of the vesicles to be examined. TEM images in Figure 19 show EVs of both spherical and irregular shapes. In some cases, even the bilipid membrane and internal structure of EVs can be distinguished. Obtained TEM images also confirm the size distribution of EVs measured with the qNano device. Although structures larger than 300 nm in diameter are also visible, mostly smaller structures can be observed. In addition, small vesicle fragments can also be distinguished. These can originate from the sample preparation process for TEM measurements but also from the isolation process.

The obtained FTIR data provided information about the biomolecular components present in the vesicles, such as lipids and proteins. The obtained spectrum indicates a very good quality of the sample, individual bands are clearly visible and no undesirable signal from water was detected. The most distinct bands in the spectrum were those for amide I and amide II. These signals arise from the vibrations of amide bonds within proteins and their analysis can help in understanding the nature of proteins present in EVs, their conformational changes, and potentially provide insights into biological processes and disease-related alterations.

The main stage of research for this thesis, however, were PALS measurements as well as a

thorough familiarisation with the possibilities and limitations of this technique and the adaptation of the apparatus.

The preparation of the PALS system described here involved numerous calibrations and test measurements. The first measurements with biological material, after the appropriate preparation of the apparatus, were conducted on pancreatic beta cells from which the EVs were isolated. The measurements were carried out at two temperatures, 22°C (room temperature) and 34.2°C (near physiological temperature). Both for cells collected straight from the cell culture and for cells that were stored frozen and thawed before the measurement, no significant differences were observed in the lifetime of positronium for different measurement temperatures. The o-Ps lifetime can be influenced by the microenvironment within cells, including the presence of cellular components, such as proteins and membranes. While temperature can affect the properties and behaviour of these components, the small temperature difference between 22°C and 34.2°C may not cause significant structural changes that would markedly alter o-Ps lifetime. In general, the o-Ps lifetime seems to be slightly higher for thawed cells (τ_{22} = 1.96 ns and τ_{34} = 1.95 ns) than for cells that were measured immediately after collection from the cell culture (τ_{22} = 1.91 ns and τ_{34} = 1.91 ns). However, this difference is not significant and a better understanding of the occurring phenomenon would require further research.

Prior to the measurement with the EV sample, o-Ps lifetime in the PBS buffer in which the vesicles were suspended was also determined. The measurements were again carried out at two different temperatures, exactly as in the case of cells. As expected, the results obtained are the same as for water (τ_{22} = 1.81 ns and τ_{34} = 1.78 ns). PBS buffer is composed of various salts and a buffering agent to maintain a stable pH. However, these components typically do not significantly affect the chemical reactivity or stability of o-Ps. Since the chemical influence of PBS components on o-Ps is minimal, the lifetime of o-Ps in PBS buffer and water should not show substantial differences. The temperature dependence characteristic for water, consistent with the literature, is visible also for the PBS buffer.

Just like in previous measurements, the EV sample was also measured at two temperatures. At 22 °C the measured mean o-Ps lifetime was 1.87 ns, whereas at 34.2 °C it was 1.83 ns. A similar relationship as in the case of water or PBS buffer can be seen here, where the lifetime o-Ps slightly decreases with increasing temperature. As shown in Figure 27, there are differences between the results for PBS and the EVs sample, but they are not significant. EVs are small entities and while these components can potentially influence the microenvironment and thus the o-Ps lifetime, their contribution may be relatively small compared to the overall volume of the buffer. Therefore, the presence of EVs in the buffer may not induce significant changes in the o-Ps lifetime unless a very

highly concentrated sample is achieved. Obtaining a highly concentrated sample of EVs from a traditional 2D cell culture medium can be challenging. The feasibility and costs of achieving high concentrations could be improved by the use of different culturing methods (such as bioreactors) and the improvement of chosen isolation and concentration methods. Optimising the process for high yield and large scale would allow the PALS technique to be applied for EV research in medicine and biology.

6. Conclusions

Given the motivation behind this thesis, the following conclusions can be drawn:

1. A successful isolation of EVs from a 2D large-scale human beta-pancreatic cell culture was achieved using the low-pressure filtration method. To assess the efficiency of the isolation process, ESEM images of the dialysis membrane were taken. Based on these results, the good performance of this experiment can be concluded.

2. Measurements based on TRPS technology yielded precise and reproducible results, enabling the determination of the size distribution and concentration of EVs.

3. The quality of the sample with isolated EVs was suitable for FTIR examinations. Obtained FTIR data provided insights into the overall biomolecular signatures of the isolated EVs.

4. TEM images revealed the presence of spherical vesicles in the sample and provided visual information about their morphology and structural features. The images also allowed for the determination of the size distribution of the EVs, providing complementary information about their dimensional range.

5. The o-Ps lifetime results in pancreatic beta cells are comparable at temperatures of 22 and 34.2 degrees Celsius, both for cells collected straight from the cell culture and for thawed cells. There were also no significant differences in o-Ps lifetime in relation to whether they were fresh or thawed cells.

6. The o-Ps lifetime in PBS is the same as in water and it shows the same temperature dependence.

7. The o-Ps lifetime signal ratio for EVs and PBS is close to 1, which is caused by an insufficiently high density of EVs in the prepared sample. This does not allow for the determination of o-Ps parameters in EVs isolated from pancreatic beta cells. The presented methodology showed that in order to measure o-Ps lifetime in EVs, it is necessary to increase EV concentration, at least 10 times. This requires the EV production efficiency and the isolation efficiency of the low-pressure filtration method to be improved.

References

[1] Stępień EŁ, Durak-Kozica M, Moskal P. Extracellular vesicles in vascular pathophysiology: beyond their molecular content. Pol Arch Intern Med. 2023 Apr 19;133(4):16483.

[2] Zapała B, Kamińska A, Piwowar M, Paziewska A, Gala-Błądzińska A, Stępień EŁ. MiRNA signature of urine extracellular vesicles shows the involvement of inflammatory and apoptotic processes in diabetic chronic kidney disease. Pharm Res. 2023 Mar 1;40(4):817–32.

[3] Kamińska A, Roman M, Wróbel A, Gala-Błądzińska A, Małecki MT Prof, Paluszkiewicz C, Stępień EŁ Prof. Raman spectroscopy of urinary extracellular vesicles to stratify patients with chronic kidney disease in type 2 diabetes. Nanomedicine. 2022 Jan;39:102468.

[4] Roman M, Kamińska A, Drożdż A, Platt M, Kuźniewski M, Małecki MT, Kwiatek WM, Paluszkiewicz C, Stępień EŁ. Raman spectral signatures of urinary extracellular vesicles from diabetic patients and hyperglycemic endothelial cells as potential biomarkers in diabetes. Nanomedicine. 2019 Apr;17:137-149.

[5] Stępień EŁ, Durak-Kozica M, Kamińska A, Targosz-Korecka M, Libera M, Tylko G, Opalińska A, Kapusta M, Solnica B, Georgescu A, Costa MC, Czyżewska-Buczyńska A, Witkiewicz W, Małecki MT, Enguita FJ. Circulating ectosomes: Determination of angiogenic microRNAs in type 2 diabetes. Theranostics. 2018 Jun 23;8(14):3874-3890.

[6] Tokarz A, Szuścik I, Kuśnierz-Cabala B, Kapusta M, Konkolewska M, Żurakowski A, Georgescu A, Stępień E. Extracellular vesicles participate in the transport of cytokines and angiogenic factors in diabetic patients with ocular complications. Folia Med Cracov. 2015;55(4):35-48.

[7] Stępień EŁ, Gruszczyński K, Kapusta P, Kowalik A, Wybrańska I. Plasma centrifugation does not influence thrombin-antithrombin and plasmin-antiplasmin levels but determines platelet microparticles count. Biochem Med (Zagreb). 2015 Jun 5;25(2):222-9.

[8] Stępień EŁ, Stankiewicz E, Zalewski J, Godlewski J, Zmudka K, Wybrańska I. Number of microparticles generated during acute myocardial infarction and stable

angina correlates with platelet activation. Arch Med Res. 2012 Jan;43(1):31-5. doi: 10.1016/j.arcmed.2012.01.006.

[9] Stepien EŁ, Rząca C, Moskal P. Novel biomarker and drug delivery systems for theranostics – extracellular vesicles. Bio-Algorithms and Med-Systems. 2021 Dec 22;17.

[10] Meldolesi J. Exosomes and Ectosomes in Intercellular Communication. Current Biology. 2018 Apr 1;28:R435–44.

[11] Stepien EŁ, Targosz-Korecka M. Microparticles in endothelial function. Postepy biochemii. 2013 Jan 1;59:395–404.

[12] Stępień EŁ, Kabłak-Ziembicka A, Czyż J, Przewłocki T, Małecki M. Microparticles, not only markers but also a therapeutic target in the early stage of diabetic retinopathy and vascular aging. Expert Opin Ther Targets. 2012 Jul;16(7):677-88.

[13] Surman M, Kędracka-Krok S, Jankowska U, Drożdż A, Stępień E, Przybyło M. Proteomic Profiling of Ectosomes Derived from Paired Urothelial Bladder Cancer and Normal Cells Reveals the Presence of Biologically-Relevant Molecules. Int J Mol Sci. 2021 Jun 24;22(13):6816.

[14] Surman M, Stępień E, Przybyło M. Melanoma-Derived Extracellular Vesicles: Focus on Their Proteome. Proteomes. 2019 May 13;7(2):21.

[15] Surman M, Stępień E, Hoja-Łukowicz D, Przybyło M. Deciphering the role of ectosomes in cancer development and progression: focus on the proteome. Clin Exp Metastasis. 2017 Apr;34(3-4):273-289.

[16] Marzec ME, Rząca C, Moskal P, Stępień EŁ. Study of the influence of hyperglycemia on the abundance of amino acids, fatty acids, and selected lipids in extracellular vesicles using TOF-SIMS. Biochemical and Biophysical Research Communications. 2022 Sep 24;622:30–6.

[17] Kalluri R, LeBleu VS. The biology, function, and biomedical applications of exosomes. Science. 2020 Feb 7;367(6478):eaau6977.

[18] Odorizzi G. The multiple personalities of Alix. J Cell Sci. 2006 Aug 1;119(Pt 15):3025-32.

[19] Ingato D, Lee JU, Sim SJ, Kwon YJ. Good things come in small packages: Overcoming challenges to harness extracellular vesicles for therapeutic delivery. J Control Release. 2016 Nov 10;241:174-185.

[20] Tokarz A, Konkolewska M, Kuśnierz-Cabala B, Maziarz B, Hanarz P, Żurakowski A, Szuścik I, Stępień EŁ. Retinopathy severity correlates with RANTES concentrations and CCR 5-positive microvesicles in diabetes. Folia Med Cracov. 2019;59(3):95-112.

[21] Kamińska A. Molecular characteristics of platelet and urinary extracellular vesicles and their possible applications in nanomedicine [Doctoral Thesis]. Krakow, Poland: Jagiellonian University; 2019.

[22] NationalNist.gov. Available from: https://www.nist.gov/laboratories/tools-instruments/positron-annihilation-lifetime-spectrometer.

[23] Jasińska B, Zgardzińska B, Chołubek G, Pietrow M, Gorgol M, Wiktor K, et al. Human tissue investigations using PALS technique - free radicals influence. Acta Phys Pol A. 2017;132(5):1556–9.

[24] Kubicz E. Biomedical applications of Positron Annihilation Lifetime Spectroscopy: nanostructural characterization of normal and cancer cells and tissues [Doctoral Thesis]. Krakow, Poland: Jagiellonian University; 2020.

[25] Bass SD, Mariazzi S, Moskal P, Stepien E. Colloquium: Positronium physics and biomedical applications. Rev Mod Phys. 2023 May;95:021002.

[26] Gidley DW, Peng H-G, Vallery RS. Positron annihilation as a method to characterize porous materials. Annu Rev Mater Res. 2006;36(1):49–79.

[27] Fong C, Dong A, Hill A, Boyd B, Drummond C. Positron annihilation lifetime spectroscopy (PALS): A probe for molecular organisation in self-assembled biomimetic systems. Physical chemistry chemical physics: PCCP. 2015 May 7;17.

[28] Han X, Gao J, Chen T, Qian L, Xiong H, Chen Z. Application progress of PALS in the correlation of structure and properties for graphene/polymer nanocomposites. Nanomaterials (Basel). 2022;12(23):4161.

[29] Moskal P, Dulski K, Chug N, Curceanu C, Czerwiński E, Dadgar M, Gajewski J, Gajos A, Grudzień G, Hiesmayr BC, Kacprzak K, Kapłon Ł, Karimi H, Klimaszewski K, Korcyl G, Kowalski P, Kozik T, Krawczyk N, Krzemień W, Kubicz

E, Małczak P, Niedźwiecki S, Pawlik-Niedźwiecka M, Pędziwiatr M, Raczyński L, Raj J, Ruciński A, Sharma S, Shivani, Shopa RY, Silarski M, Skurzok M, Stępień EŁ, Szczepanek M, Tayefi F, Wiślicki W. Positronium imaging with the novel multiphoton PET scanner. Sci Adv. 2021 Oct 15;7(42):eabh4394.

[30] Moskal P, Kubicz E, Grudzień G, Czerwiński E, Dulski K, Leszczynski B, et al. Developing a novel positronium biomarker for cardiac myxoma imaging. EJNMMI Physics. 2023 Mar 24;10.

[31] McCluskey JT, Hamid M, Guo-Parke H, McClenaghan NH, Gomis R, Flatt PR. Development and functional characterization of insulin-releasing human pancreatic beta cell lines produced by electrofusion. J Biol Chem. 2011;286(25):21982–92.

[32] Stępień EŁ, Kamińska A, Surman M, Karbowska D, Wróbel A, Przybyło M. Fourier-Transform InfraRed (FT-IR) spectroscopy to show alterations in molecular composition of EV subpopulations from melanoma cell lines in different malignancy. Biochem Biophys Rep. 2021 Jan 4;25:100888.

[33] Kamińska A, Platt M, Kasprzyk J, Kuśnierz-Cabala B, Gala-Błądzińska A, Woźnicka O, et al. Urinary extracellular vesicles: Potential biomarkers of renal function in diabetic patients. J Diabetes Res. 2016;2016:5741518.

[34] IZON Science. qNano User Manual. Available from: https://support.izon.com/reference-material-qnano-user-manual.

[35] Pennycook Gerald SJ, Liedl L, Wyder P. Encyclopedia of Condensed Matter Physics. Elsevier; 2005.

[36] Kazarian SG, Chan KL. ATR-FTIR spectroscopic imaging: recent advances and applications to biological systems. Analyst. 2013 Apr 7;138(7):1940-51.

[37] Moskal P, Jasińska B, Stępień EŁ, Bass SD. Positronium in medicine and biology. Nat Rev Phys. 2019;1(9):527–9.

[38] Palacio C. Some effects on polymers of low-energy implanted positrons. 2008.

[39] National Nuclear Data Center. Available from: http://http://www.nndc.bnl.gov.

[40] Dulski K, collaboration, on. PALS avalanche - A new PAL spectra analysis software. Acta Physica Polonica A. 2020 Feb 1;137:167–70.

List of Figures

List of Tables